Electronic Supplementary Material (ESI) for Dalton Transactions

Supporting Information

Group (IV) complexes containing the benzotriazole phenoxide ligand as catalysts for the ring-opening polymerization of lactides, epoxides and as precatalysts for the polymerization of ethylene

Sreenath Pappuru, Eswara Rao Chokkapu, Debashis Chakraborty* and Venkatachalam Ramkumar

Department of Chemistry, Indian Institute of Technology Madras, Chennai-600 036, Tamil Nadu, India. E-mail: dchakraborty@iitm.ac.in; Fax: +914422574202; Tel: +914422574223

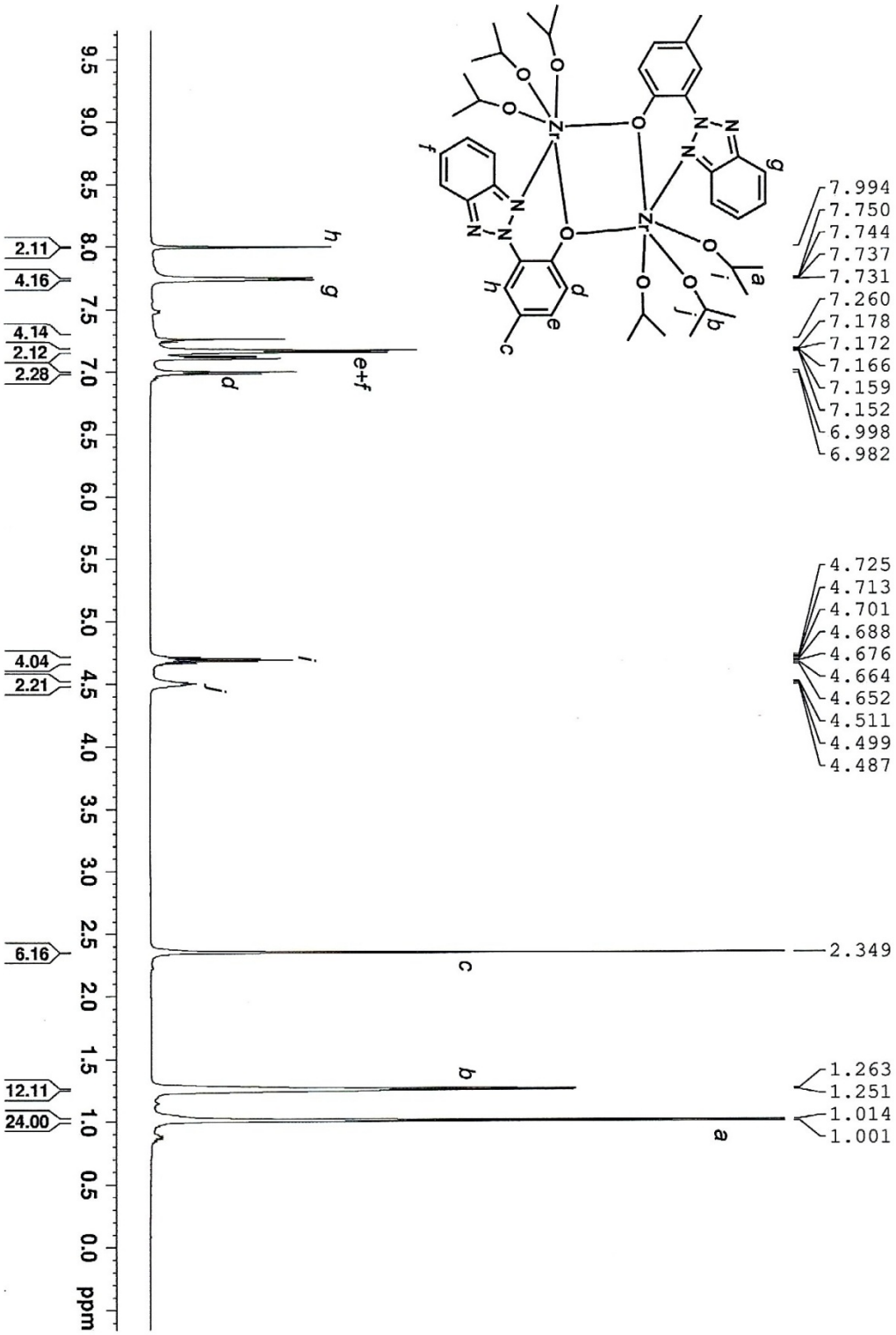

Fig. S1. ^{1}H NMR (500 MHz, $CDCl_3$) of Compound **1**

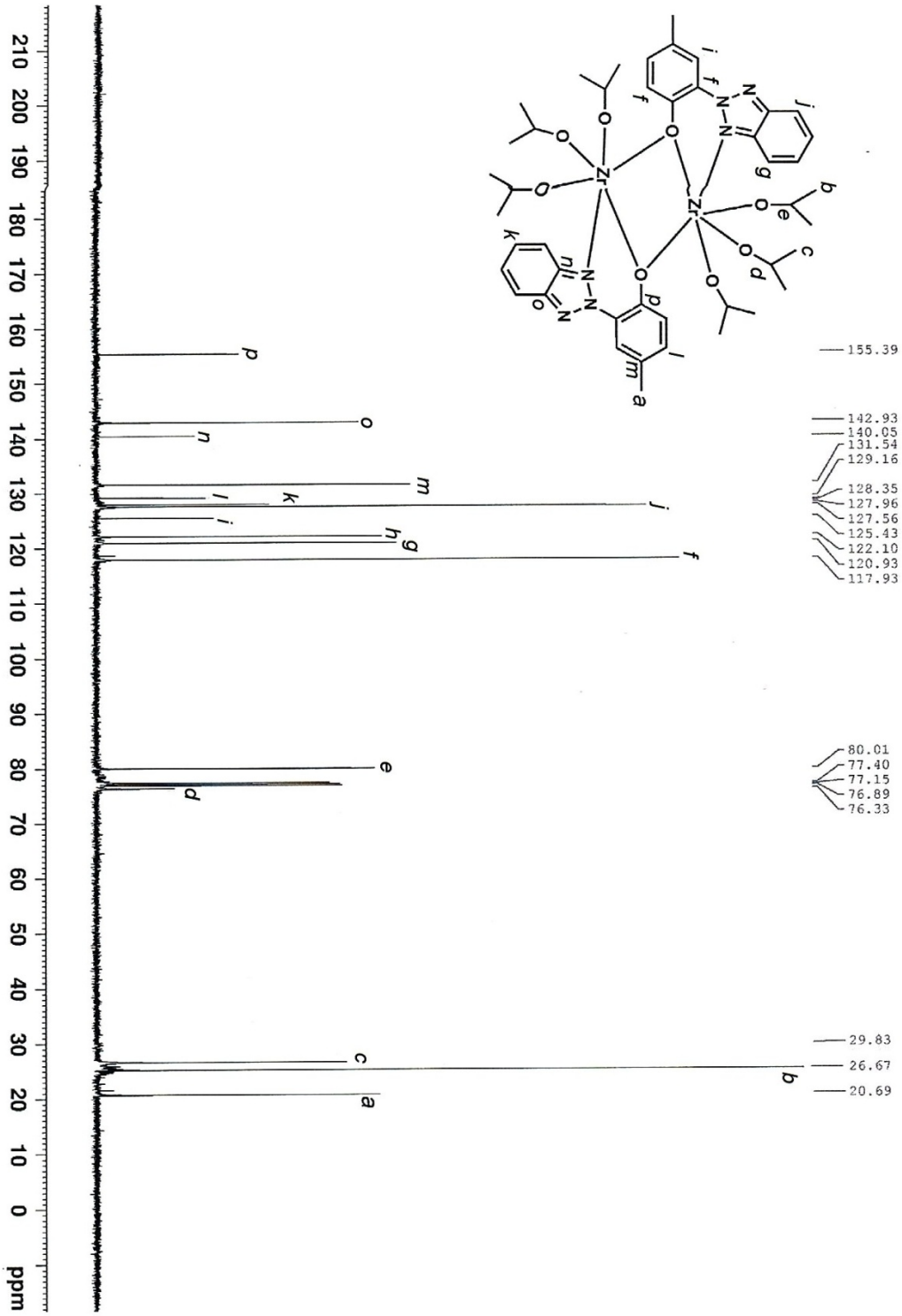

Fig. S2. ^{13}C NMR (125 MHz, $CDCl_3$) of Compound **1**

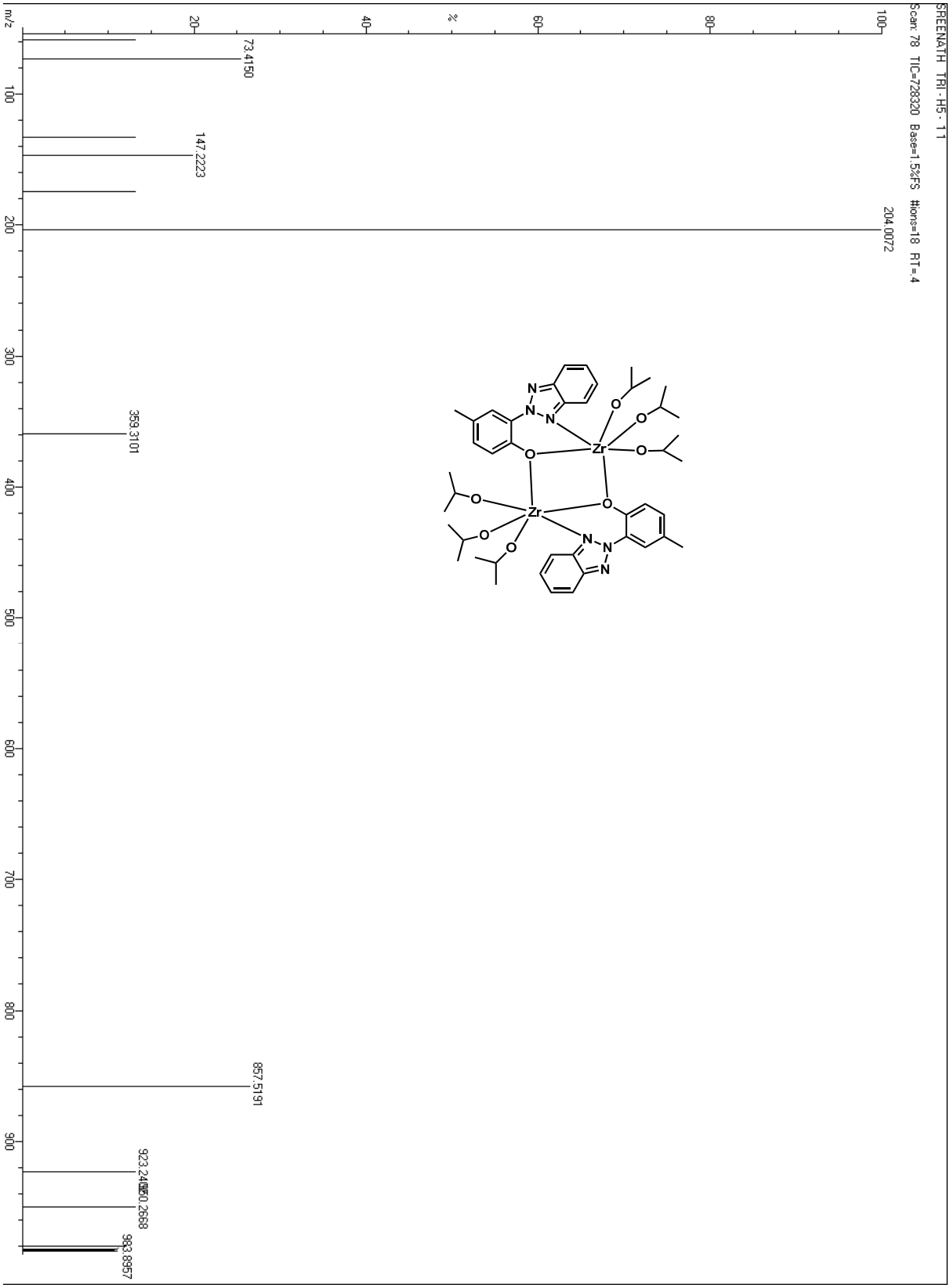

Fig. S3. ESI-Mass Spectrum of Compound **1**

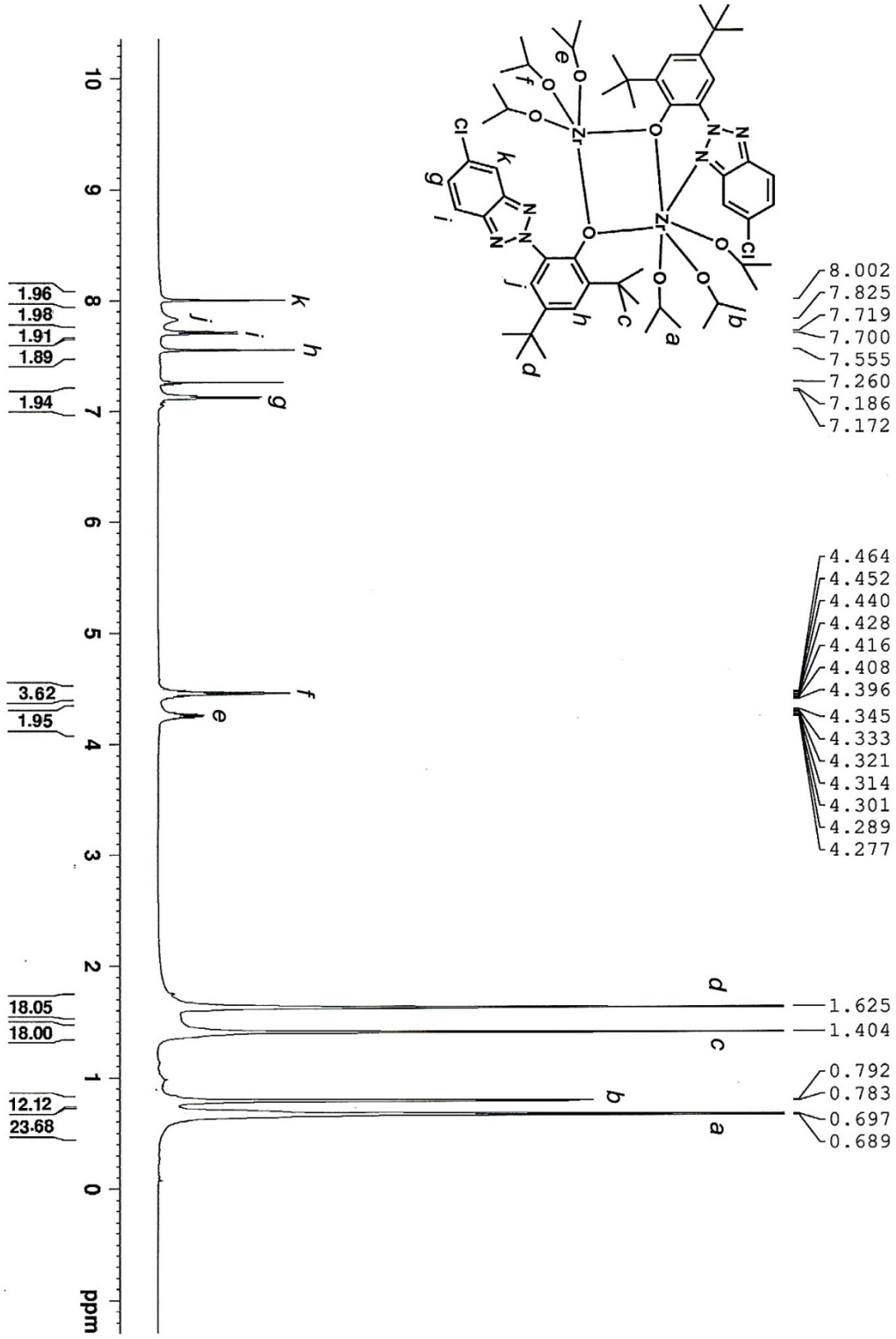

Fig. S4. ^{1}H NMR (500 MHz, $CDCl_3$) of Compound **2**

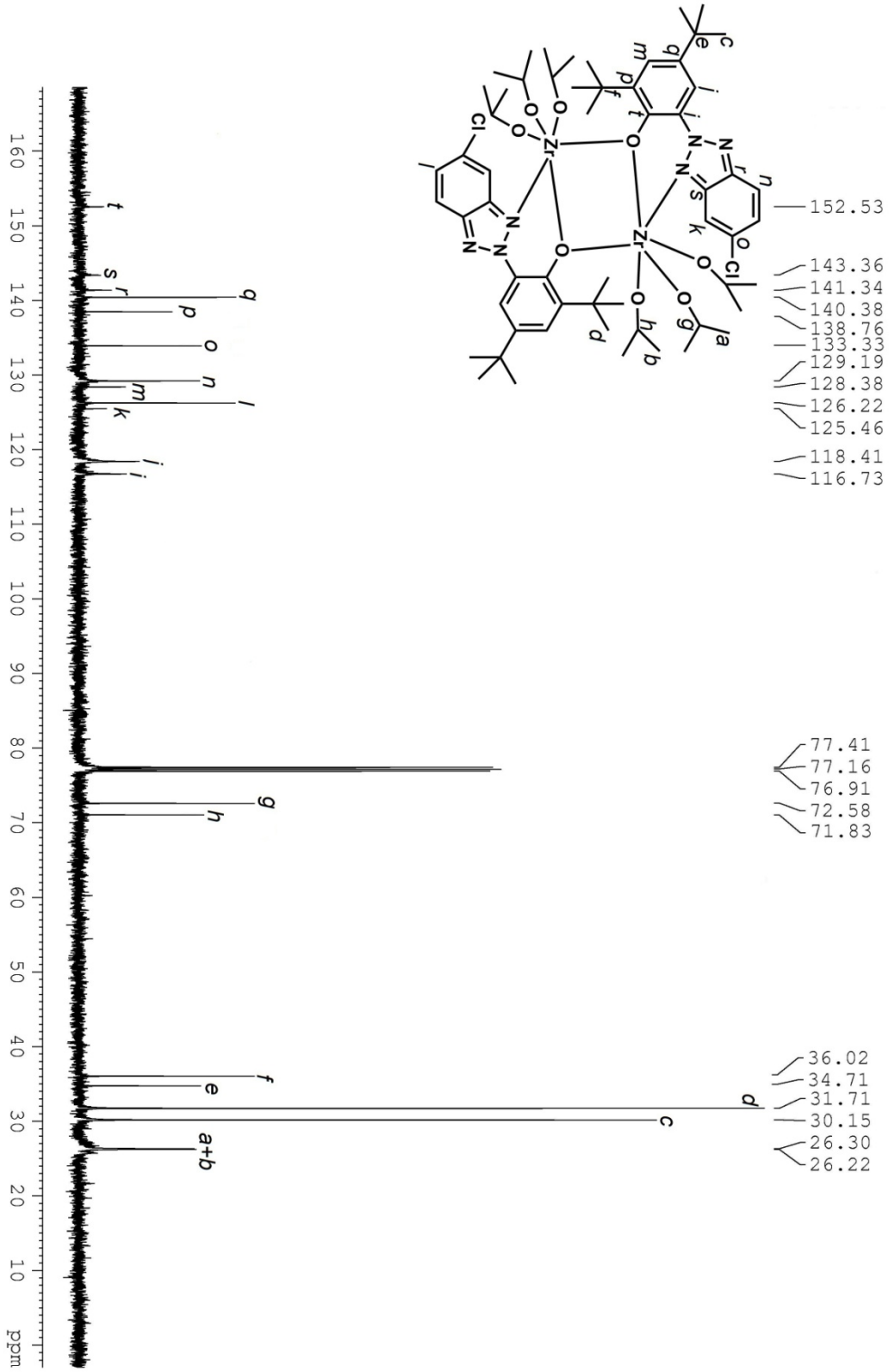

Fig. S5. ^{13}C NMR (125 MHz, $CDCl_3$) of Compound **2**

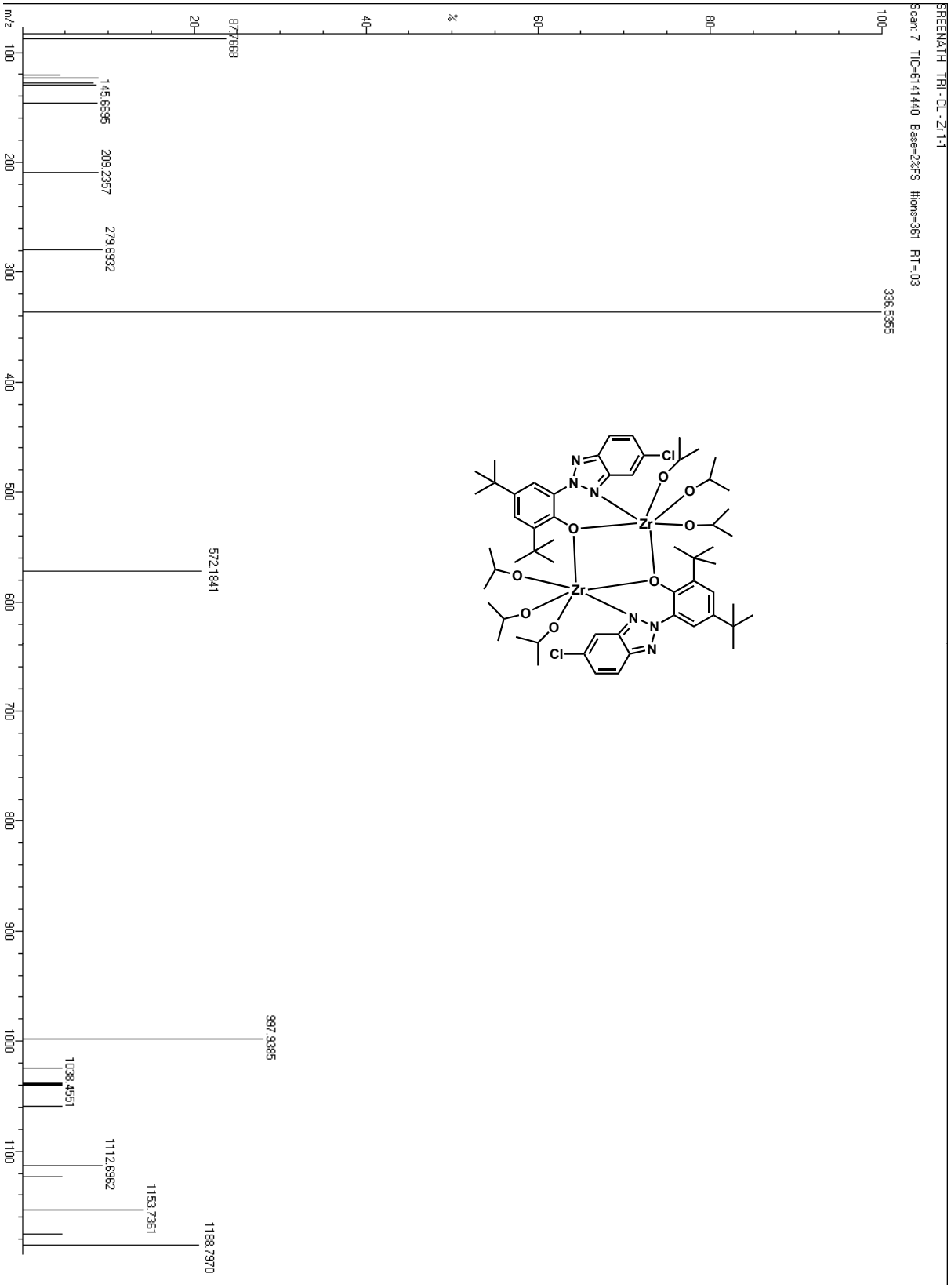

Fig. S6. ESI-Mass Spectrum of Compound **2**

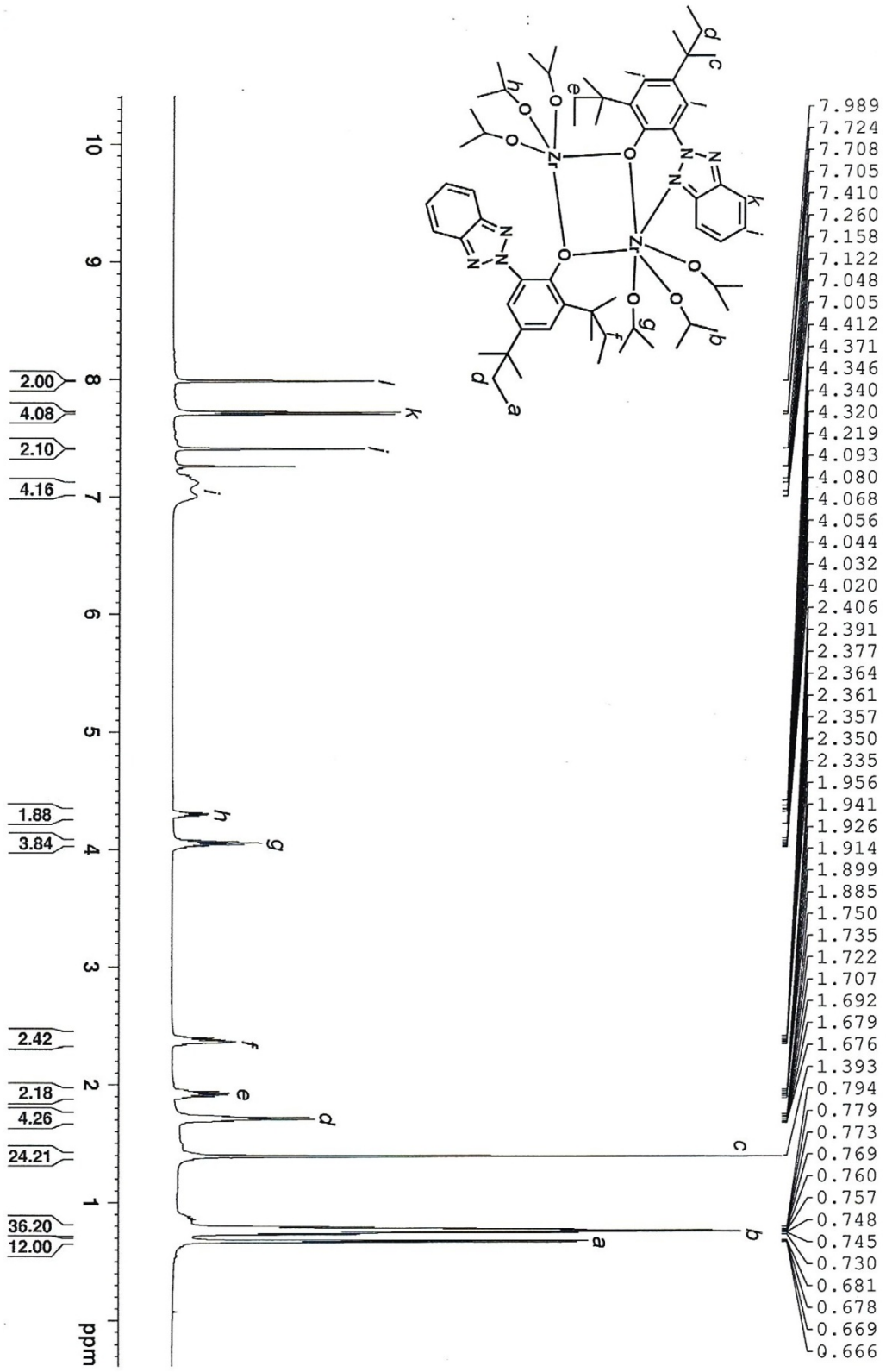

Fig. S7. ^{1}H NMR (500 MHz, $CDCl_3$) of Compound **3**

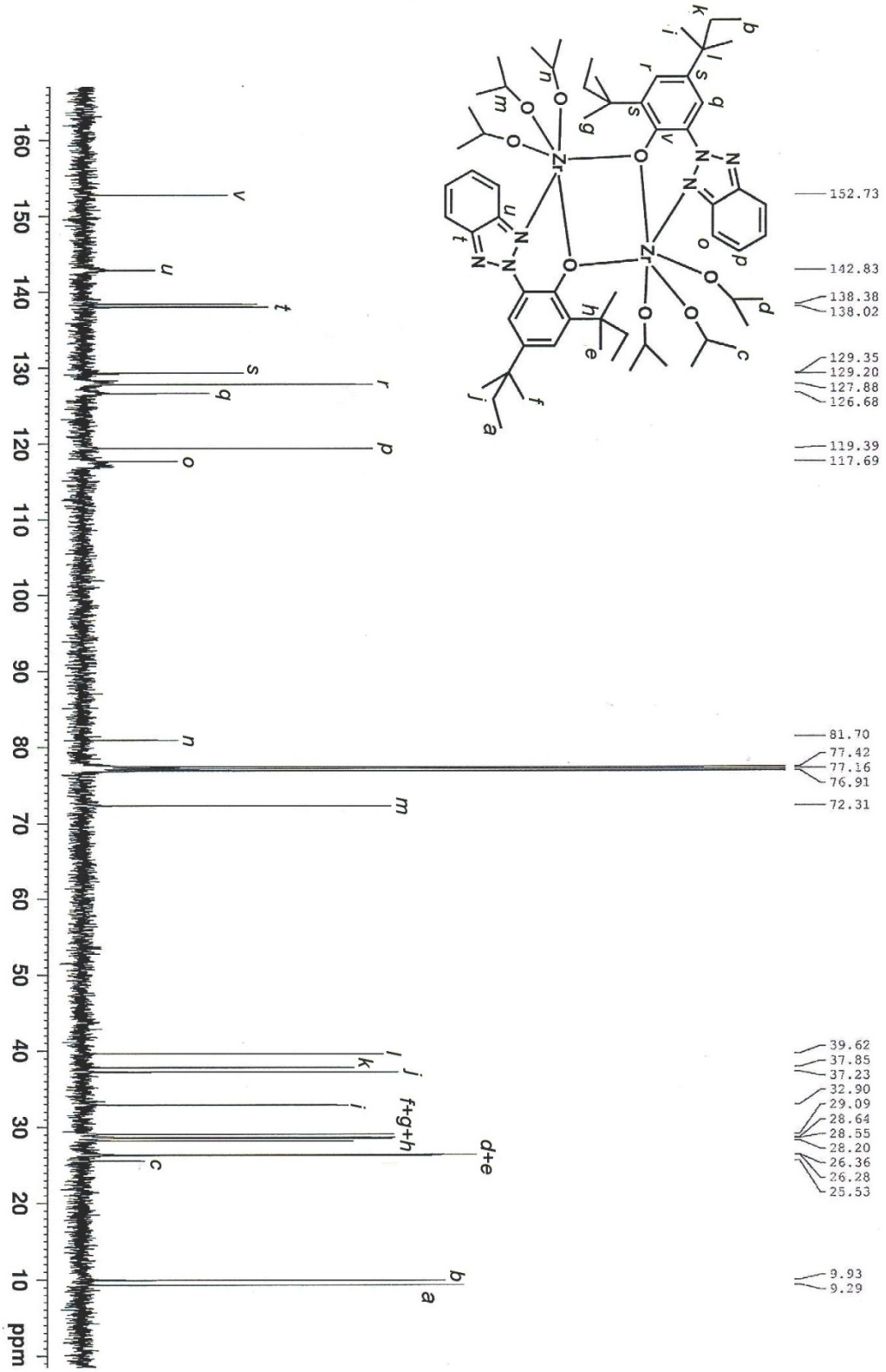

Fig. S8. ^{13}C NMR (125 MHz, $CDCl_3$) of Compound **3**

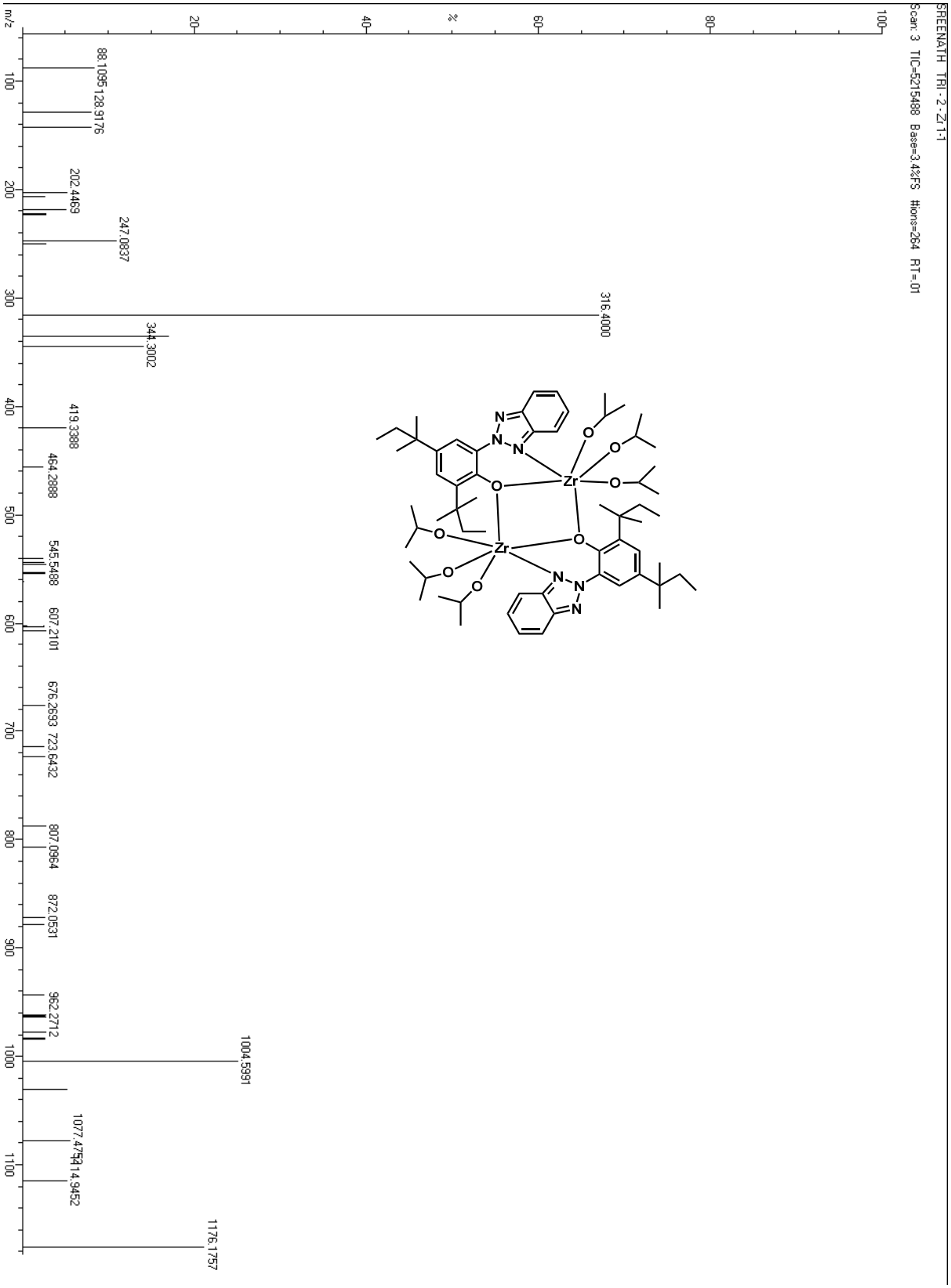

Fig. S9. ESI-Mass Spectrum of Compound **3**

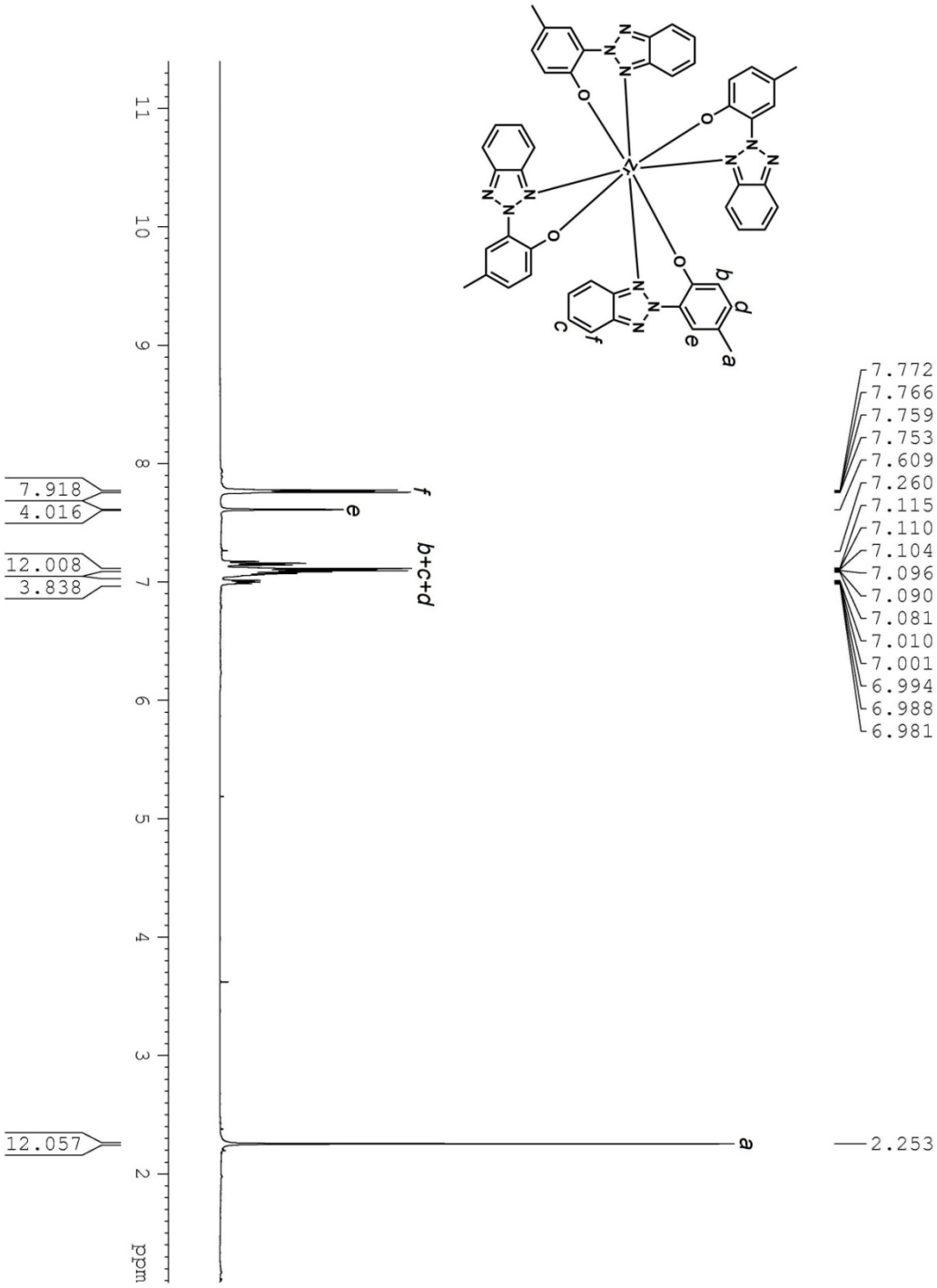

Fig. S10. ^{1}H NMR (500 MHz, $CDCl_3$) of Compound **4**

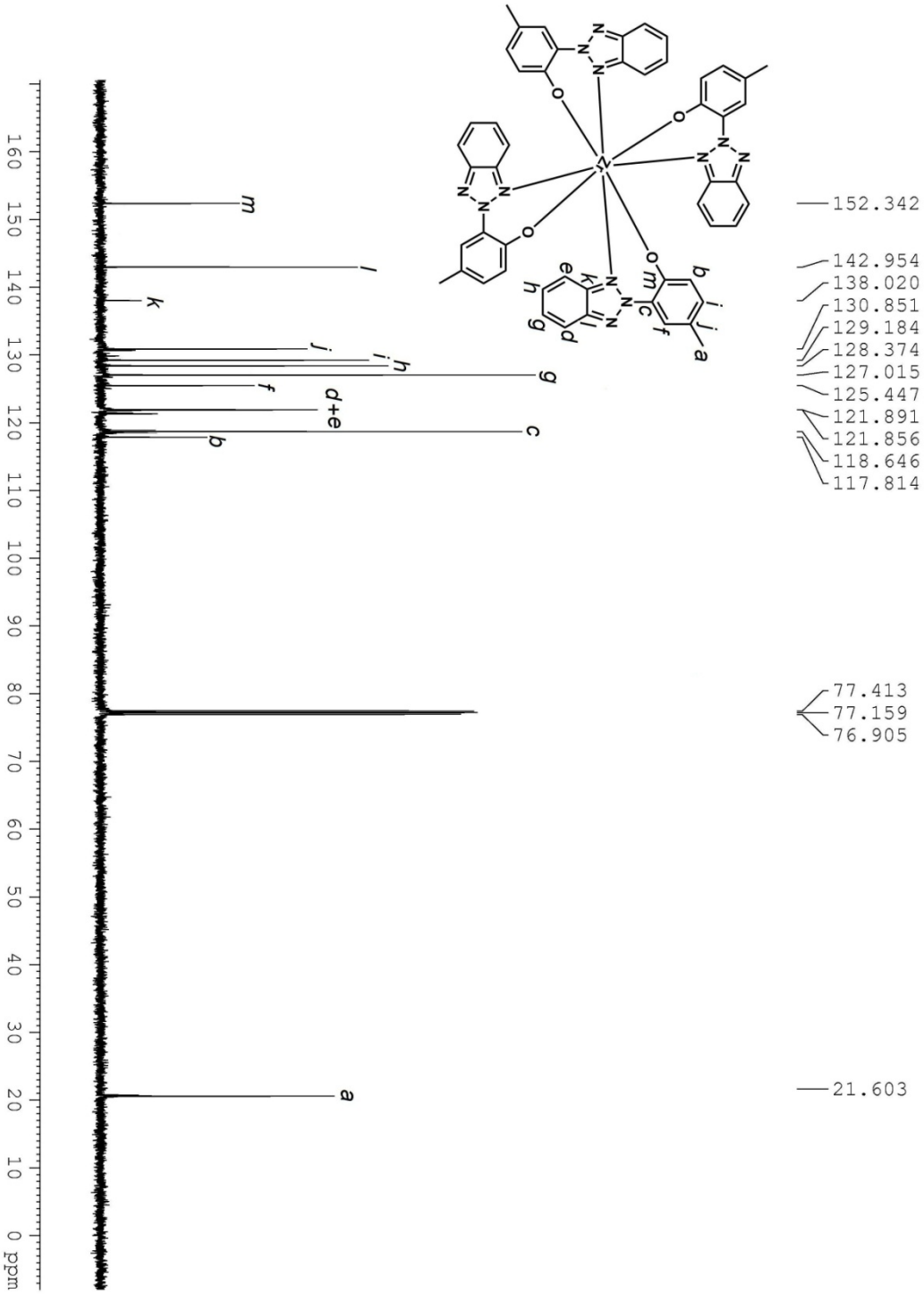

Fig. S11. ^{13}C NMR (125 MHz, $CDCl_3$) of Compound **4**

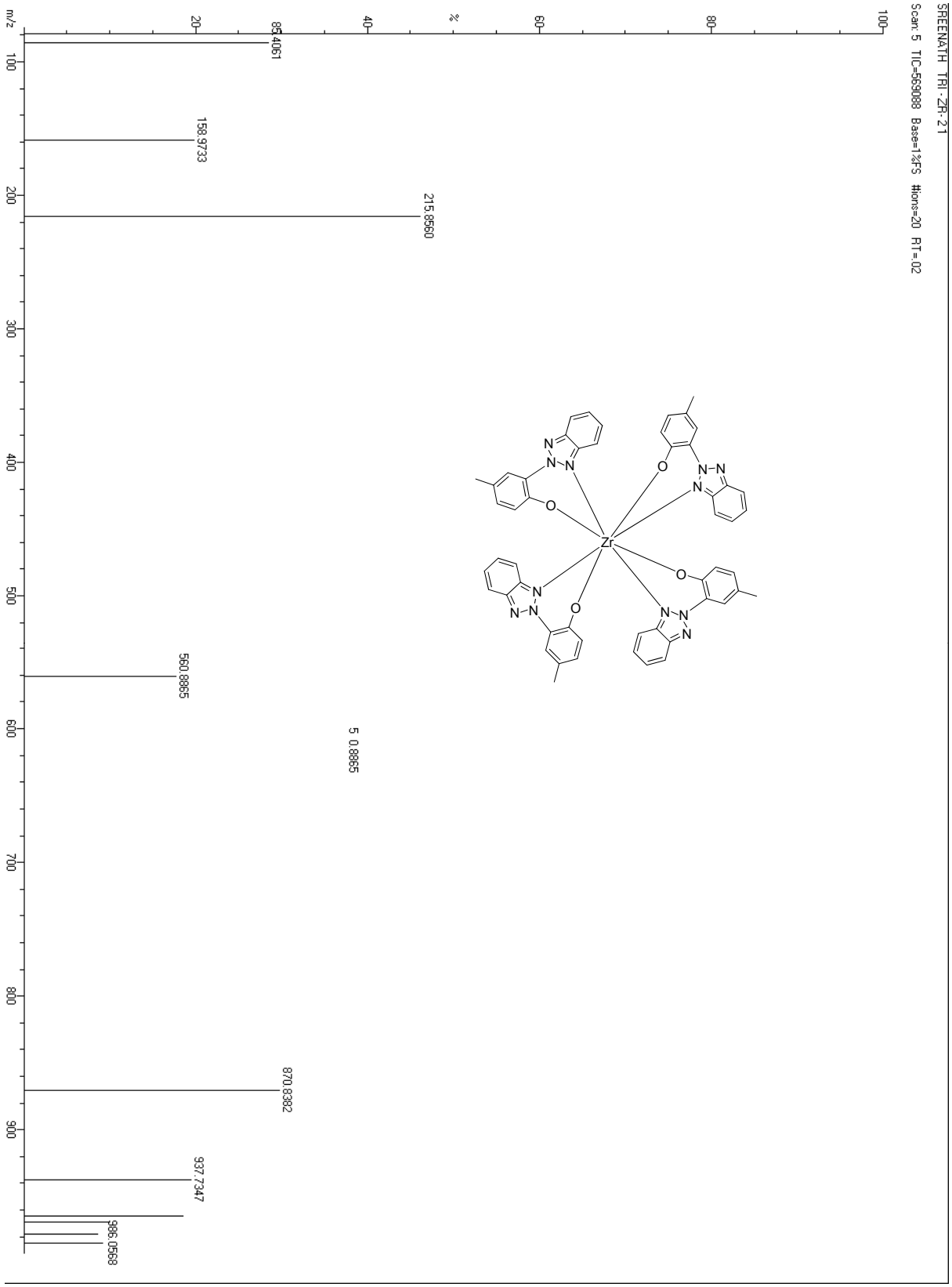

Fig. S12. ESI-Mass Spectrum of Compound **4**

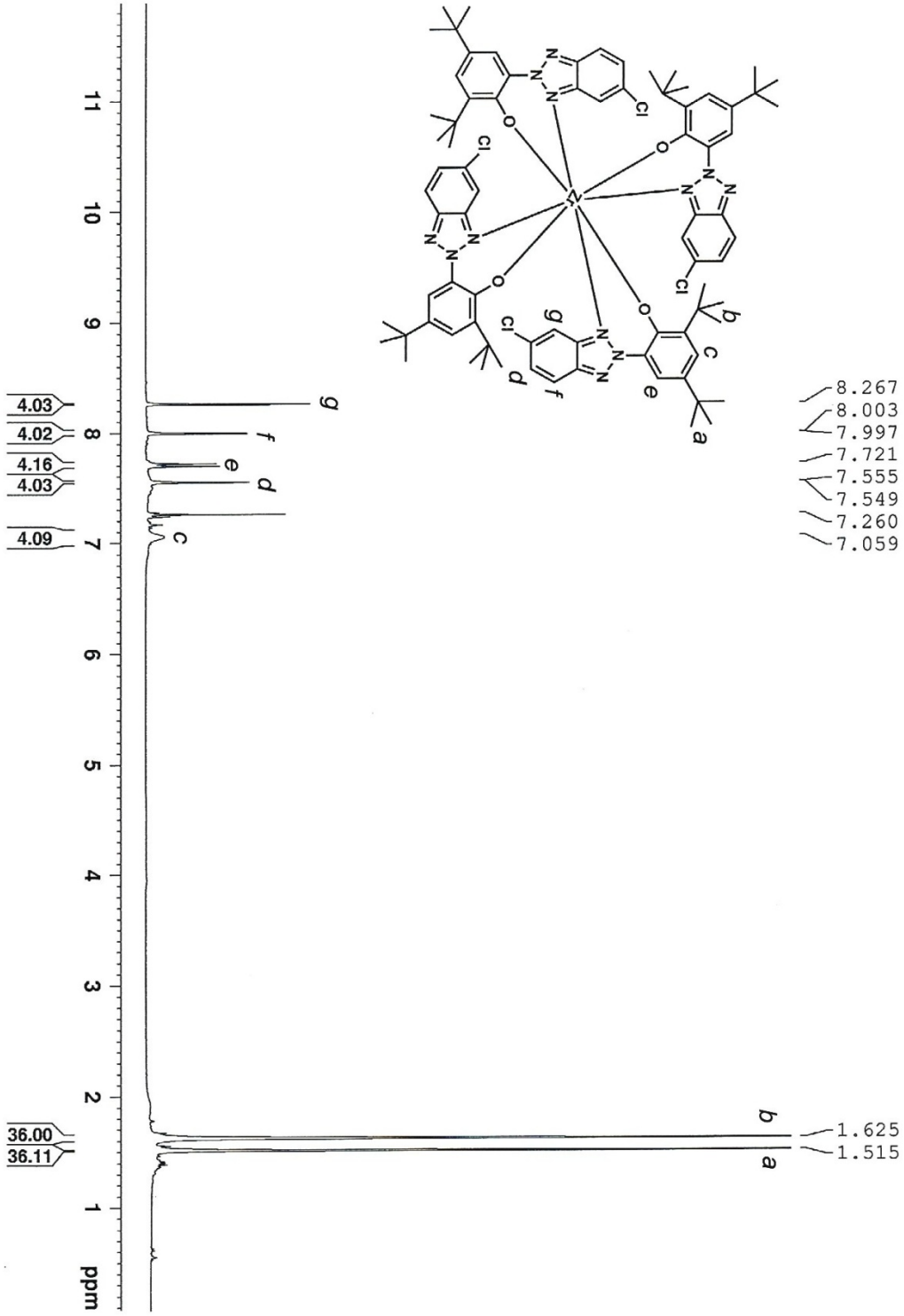

Fig. S13. ^{1}H NMR (500 MHz, $CDCl_3$) of Compound **5**

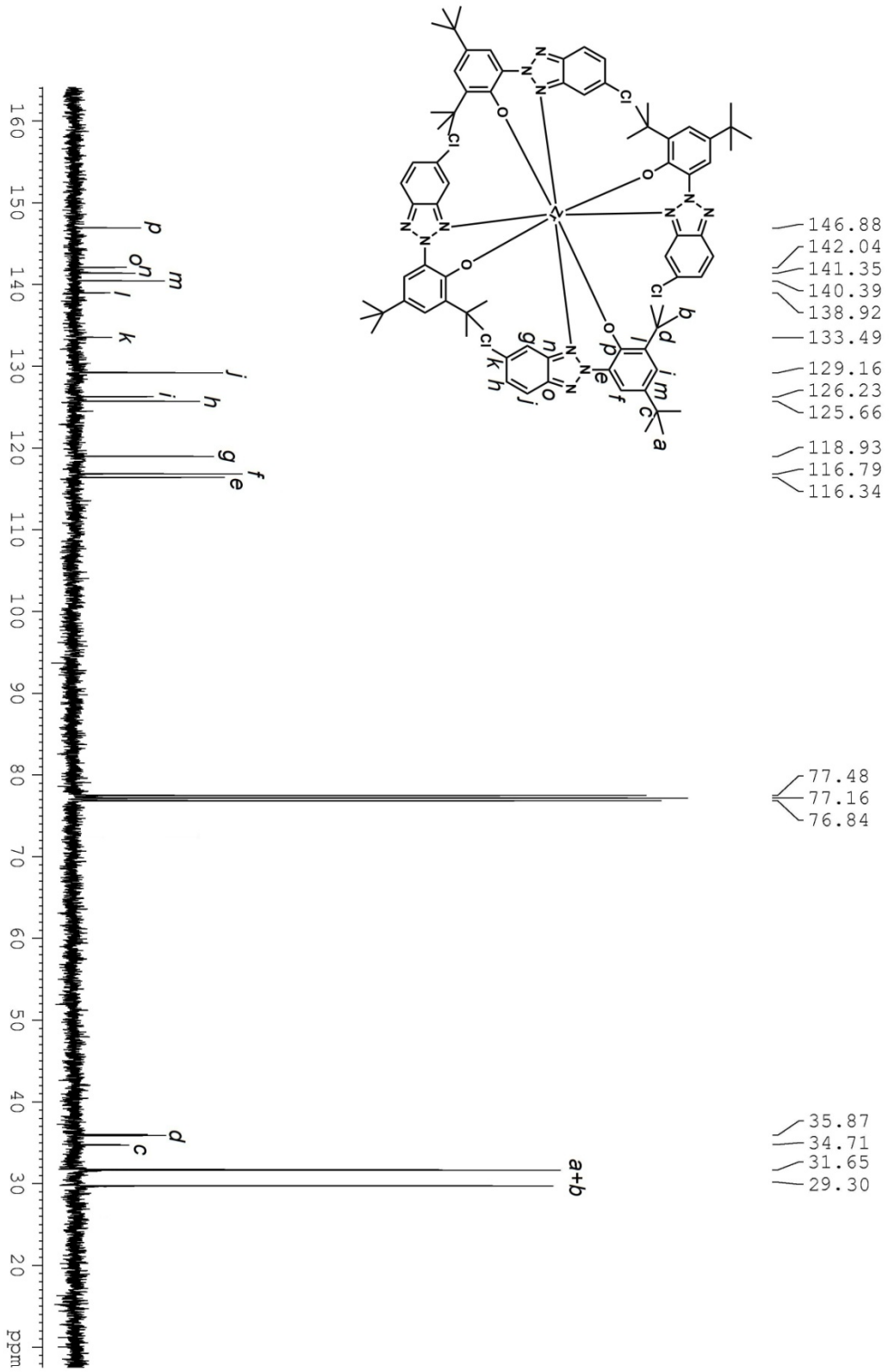

Fig. S14. ^{13}C NMR (125 MHz, $CDCl_3$) of Compound **5**

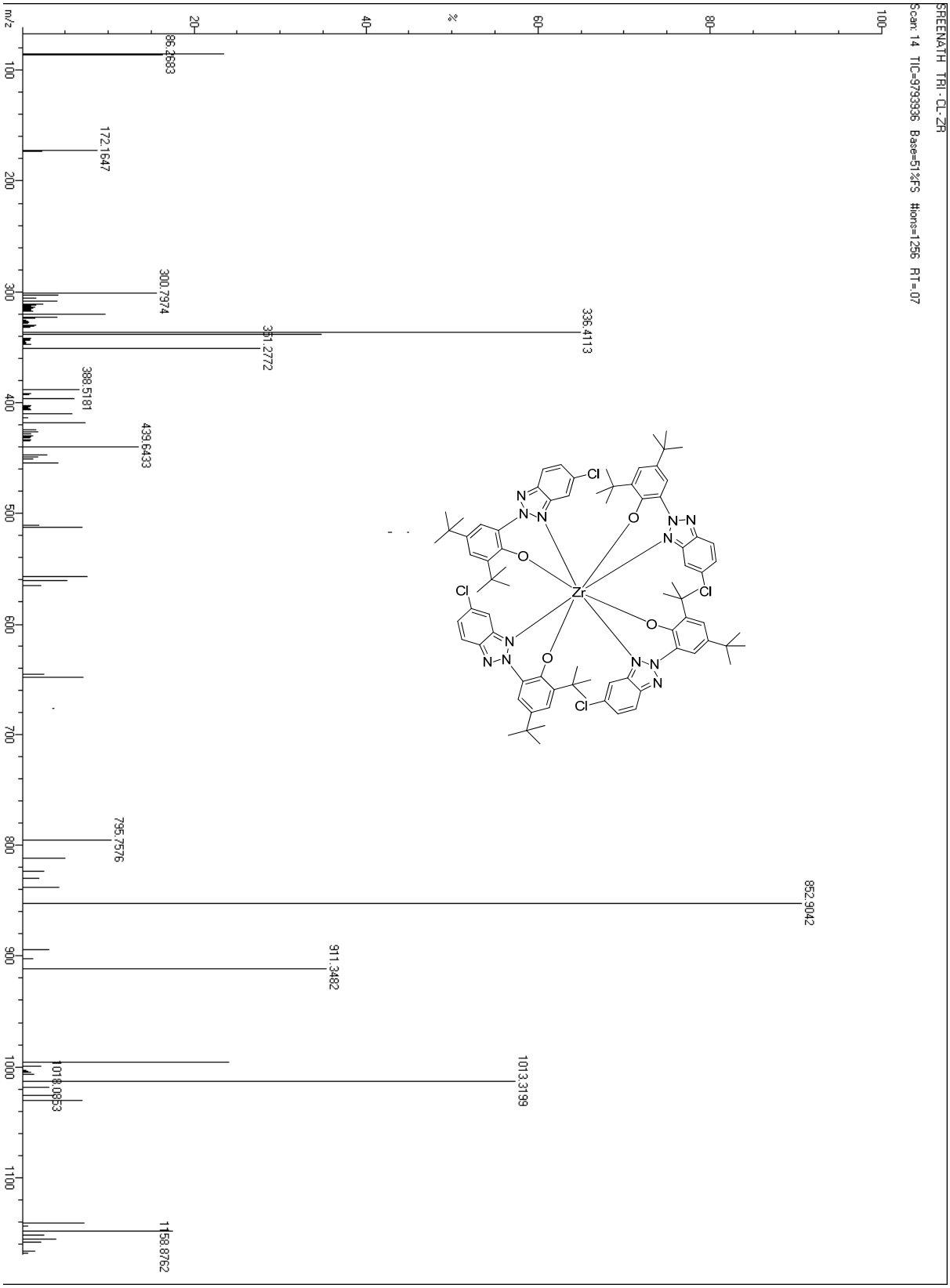

Fig. S15. ESI-Mass Spectrum of Compound **5**

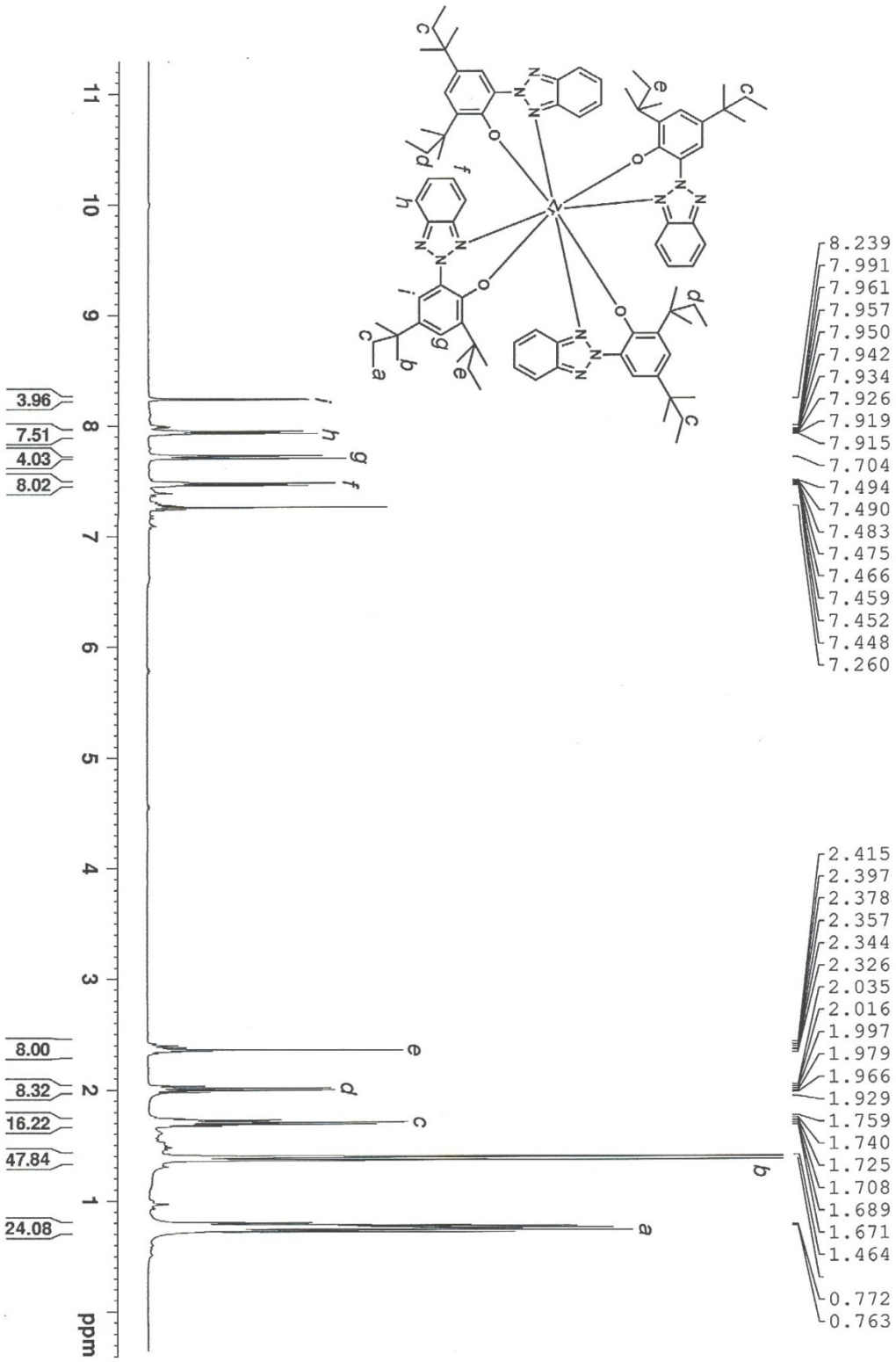

Fig. S16. ^{1}H NMR (500 MHz, $CDCl_3$) of Compound **6**

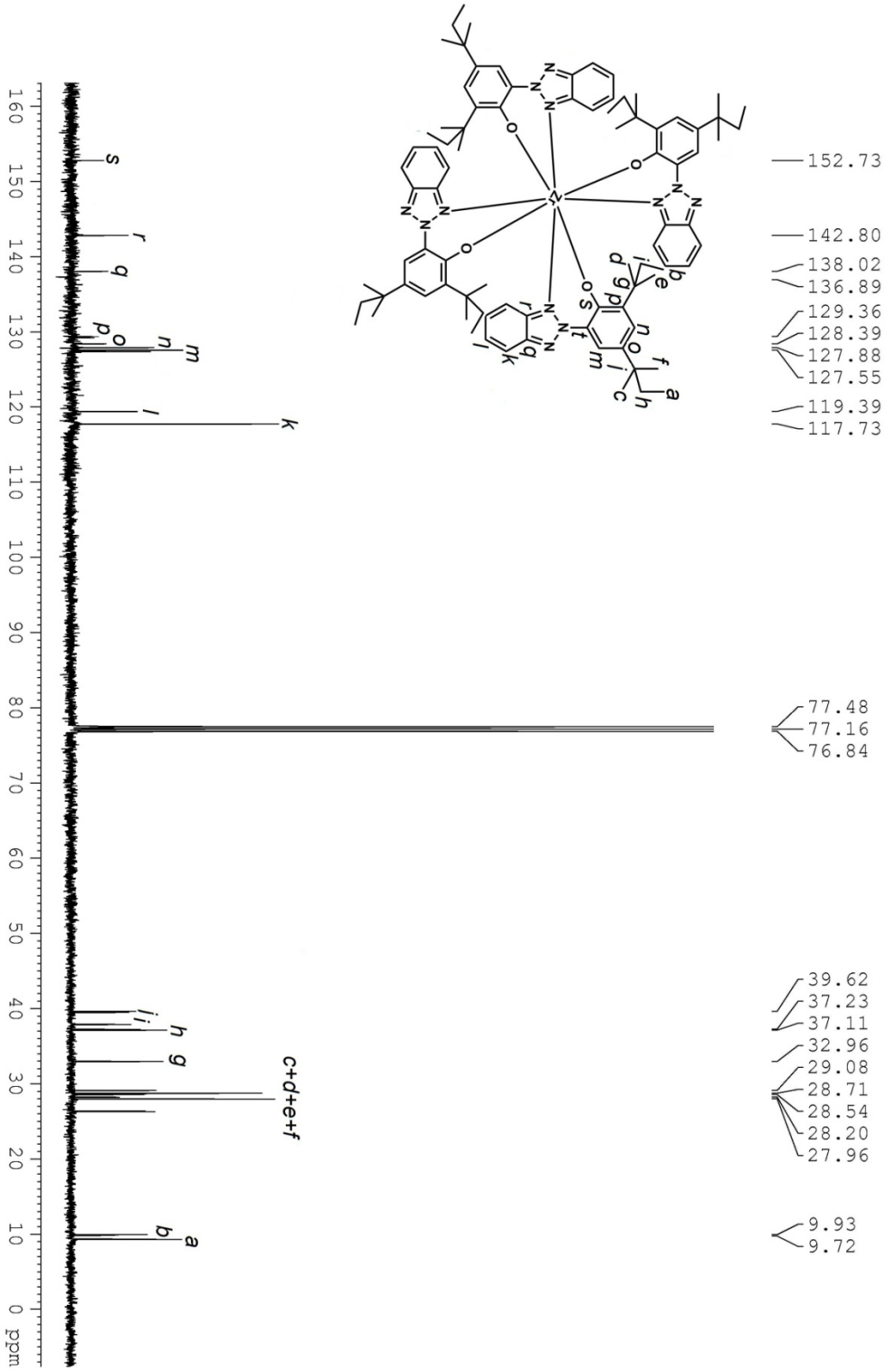

Fig. S17. ^{13}C NMR (125 MHz, $CDCl_3$) of Compound **6**

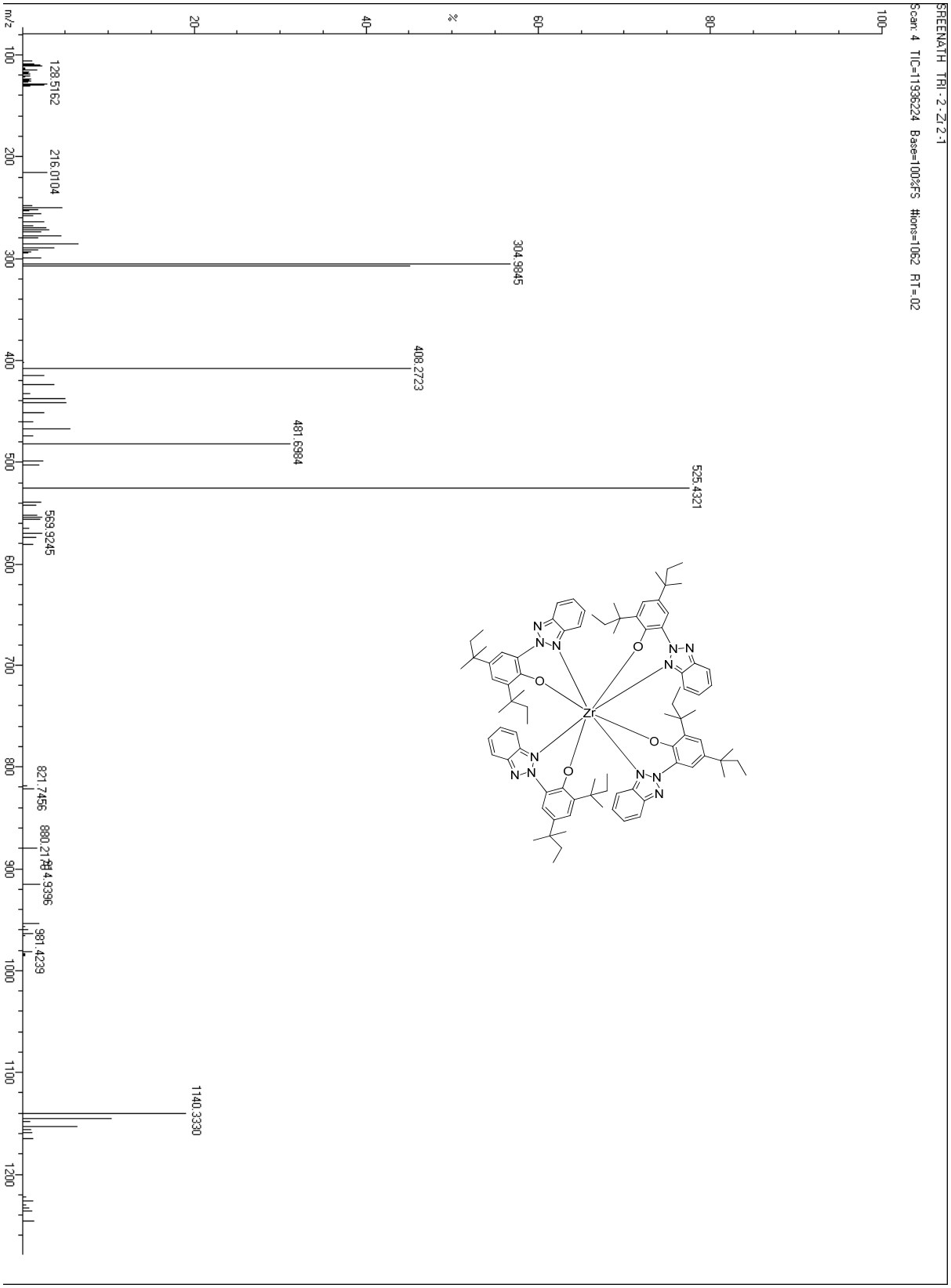

Fig. S18. ESI-Mass Spectrum of Compound **6**

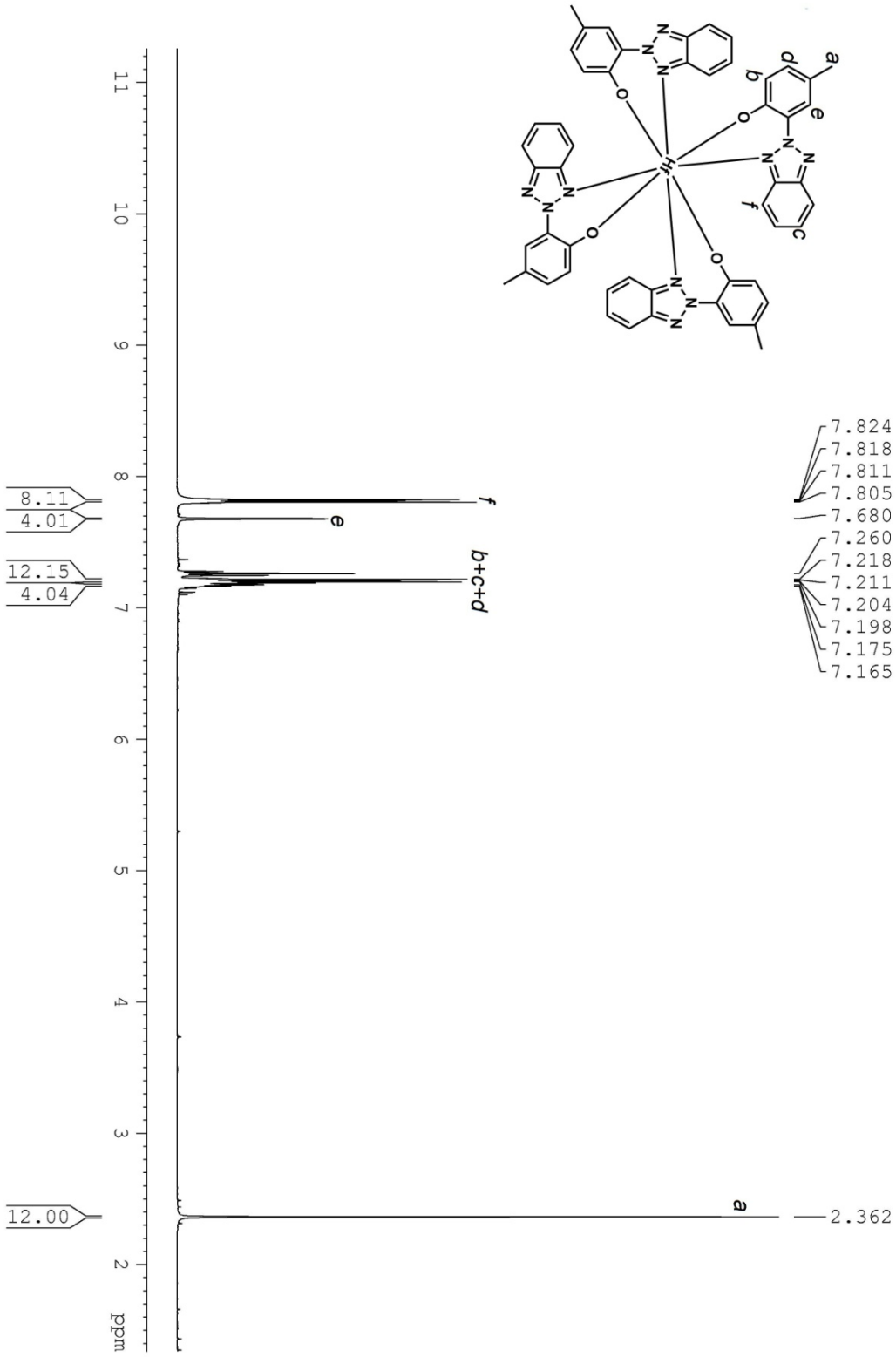

Fig. S19. ^{1}H NMR (500 MHz, $CDCl_3$) of Compound **7**

Fig. S20. ^{13}C NMR (125 MHz, $CDCl_3$) of Compound **7**

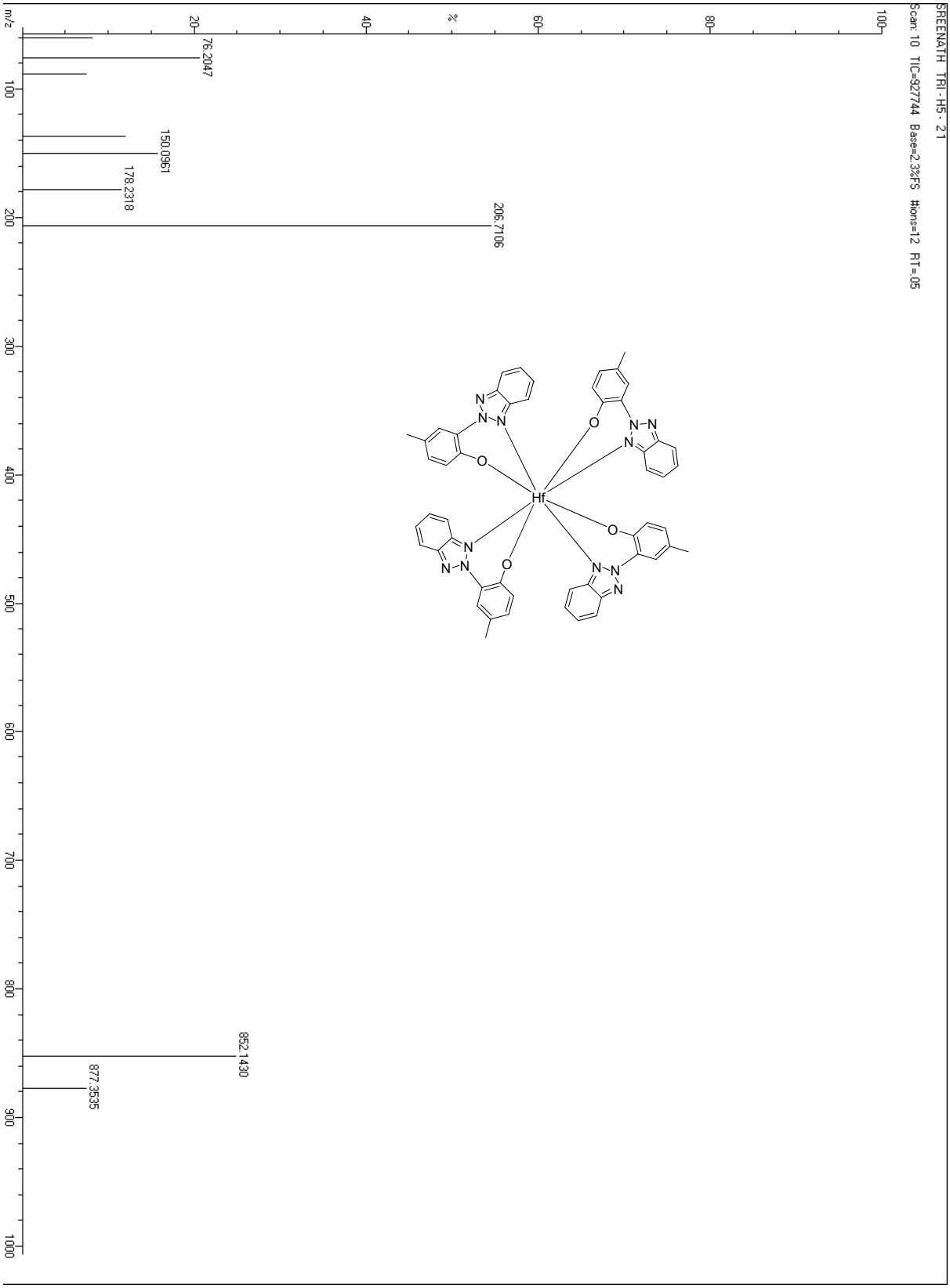

Fig. S21. ESI-Mass Spectrum of Compound **7**

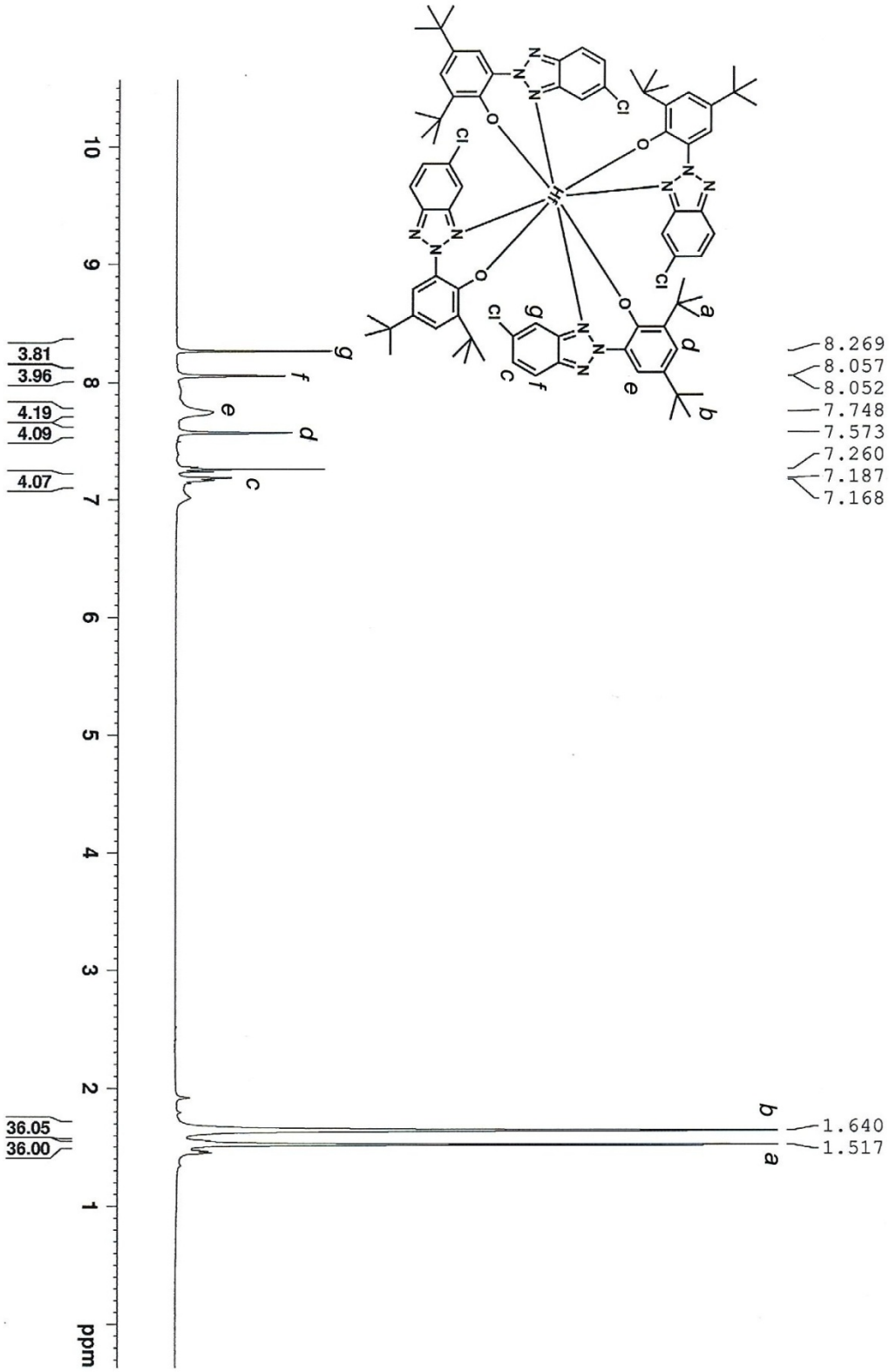

Fig. S22. ^{1}H NMR (500 MHz, $CDCl_3$) of Compound **8**

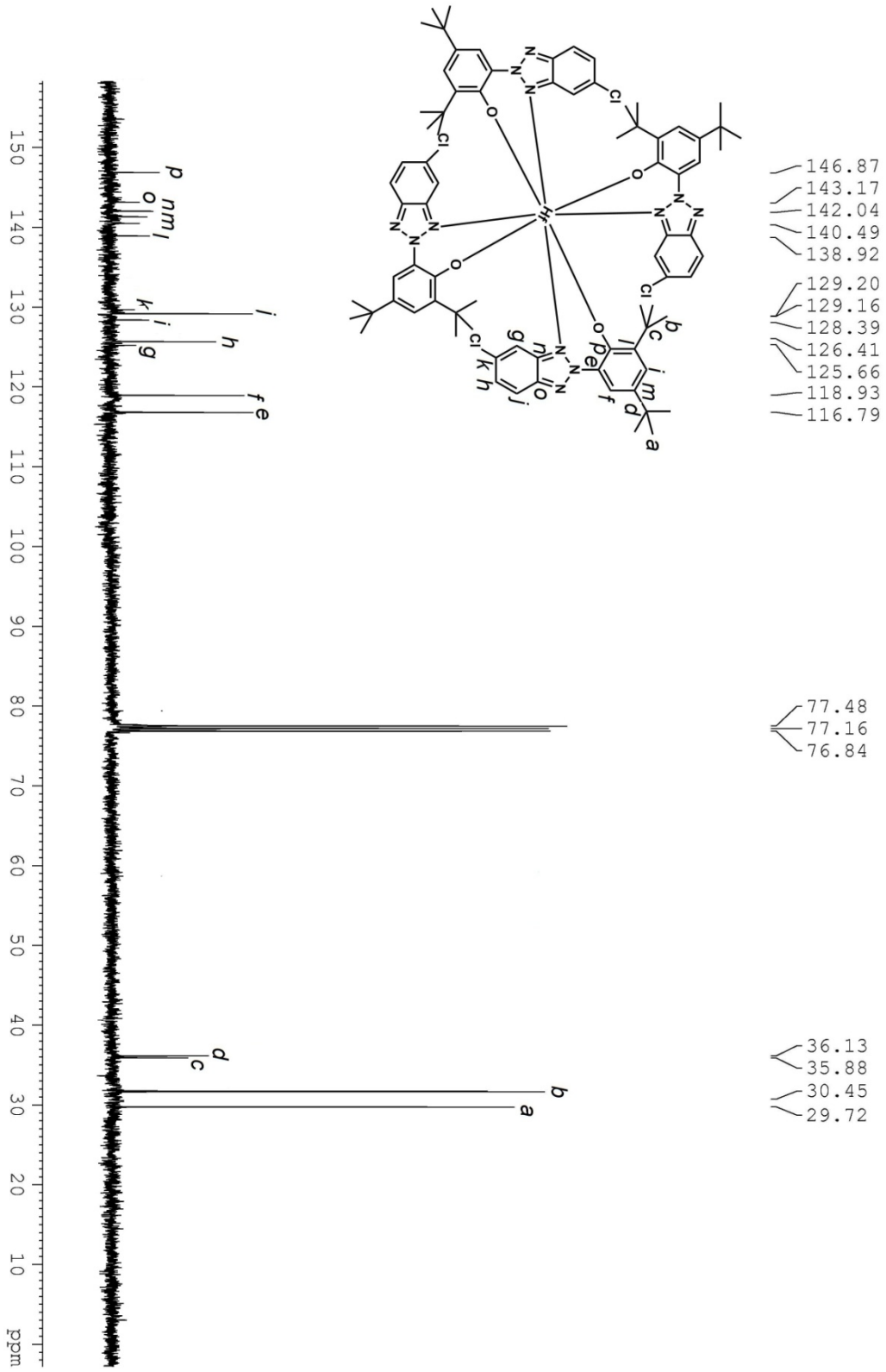

Fig. S23. ^{13}C NMR (125 MHz, $CDCl_3$) of Compound **8**

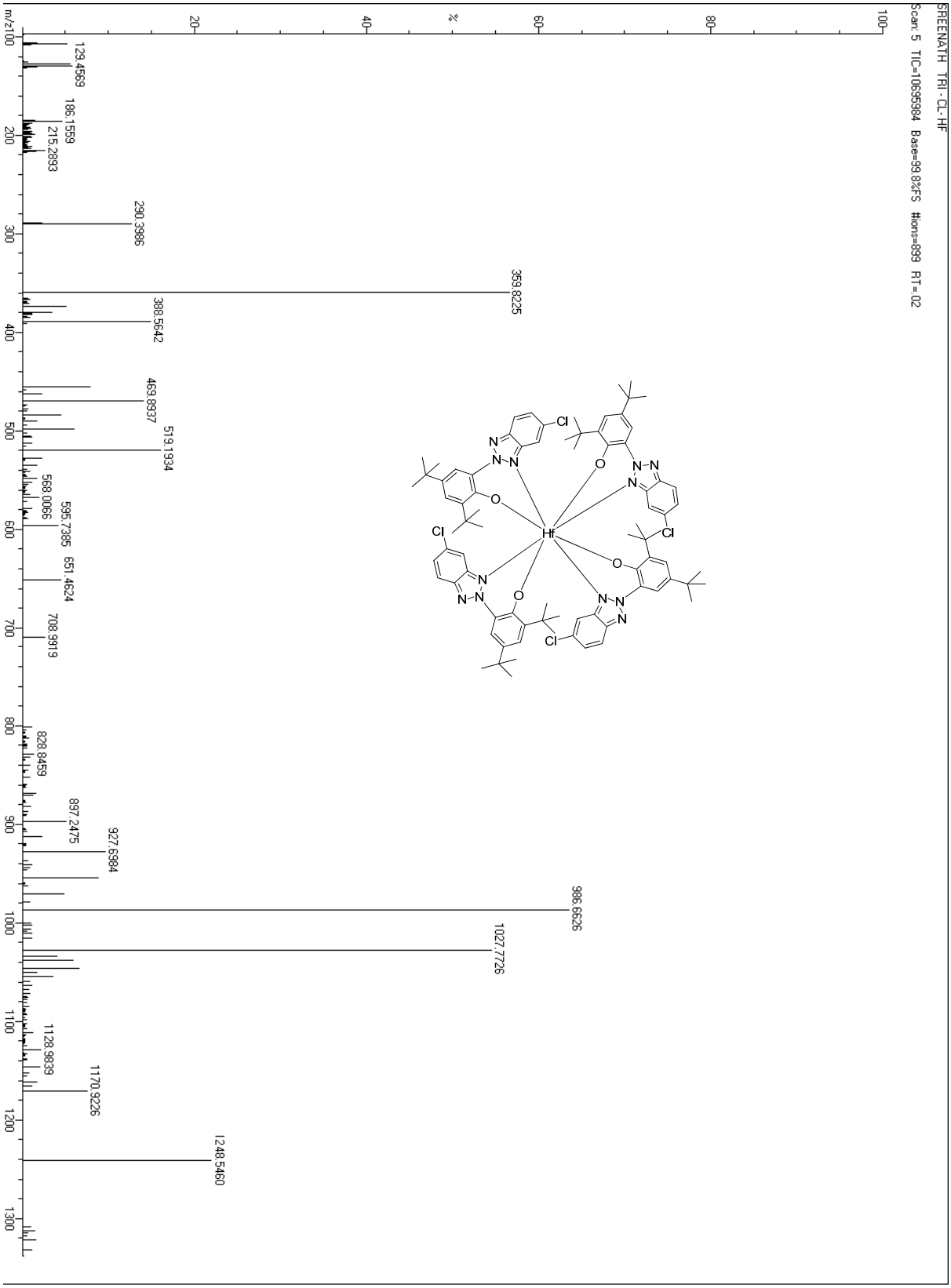

Fig. S24. ESI-Mass Spectrum of Compound **8**

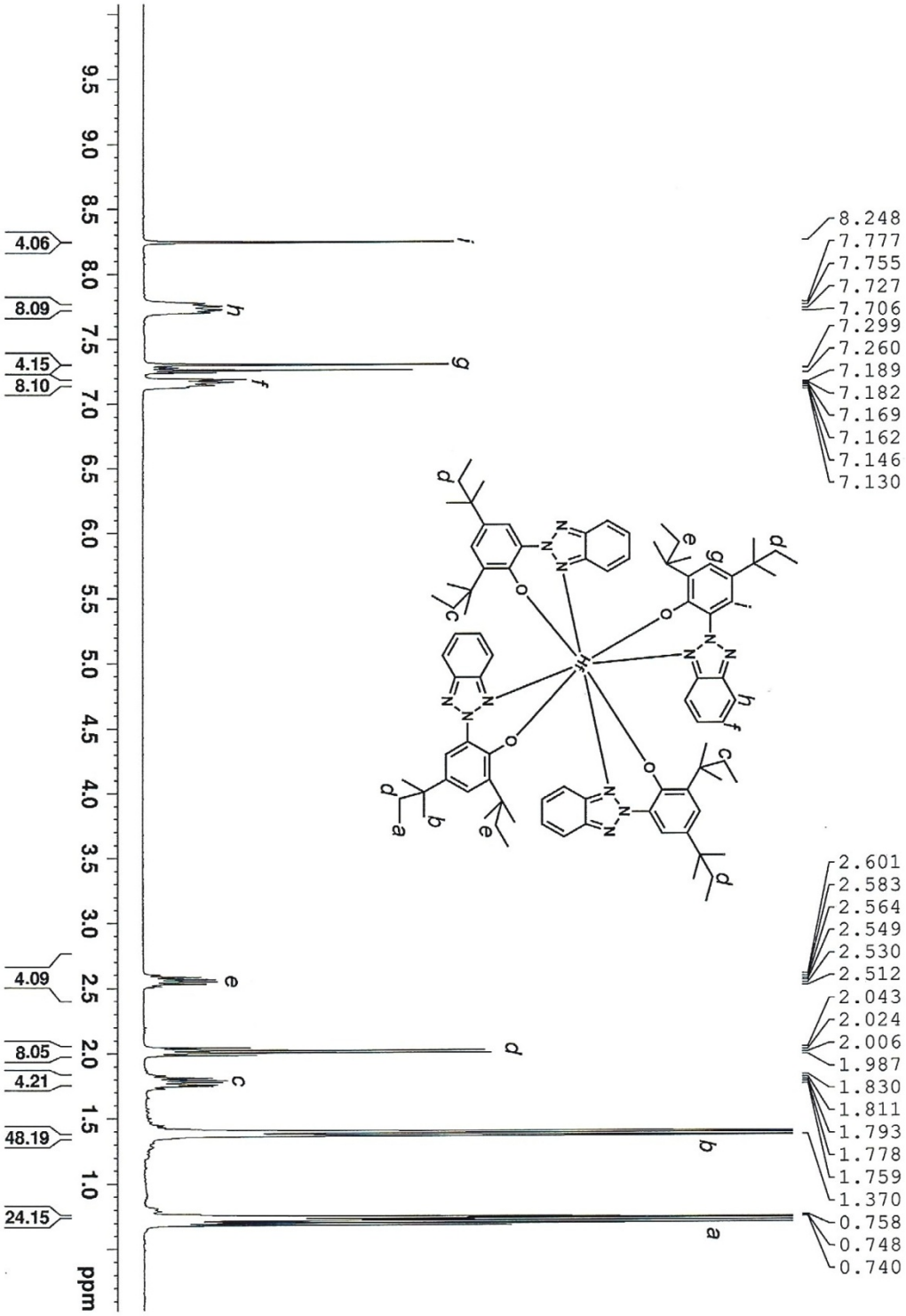

Fig. S25. ^{1}H NMR (500 MHz, $CDCl_3$) of Compound **9**

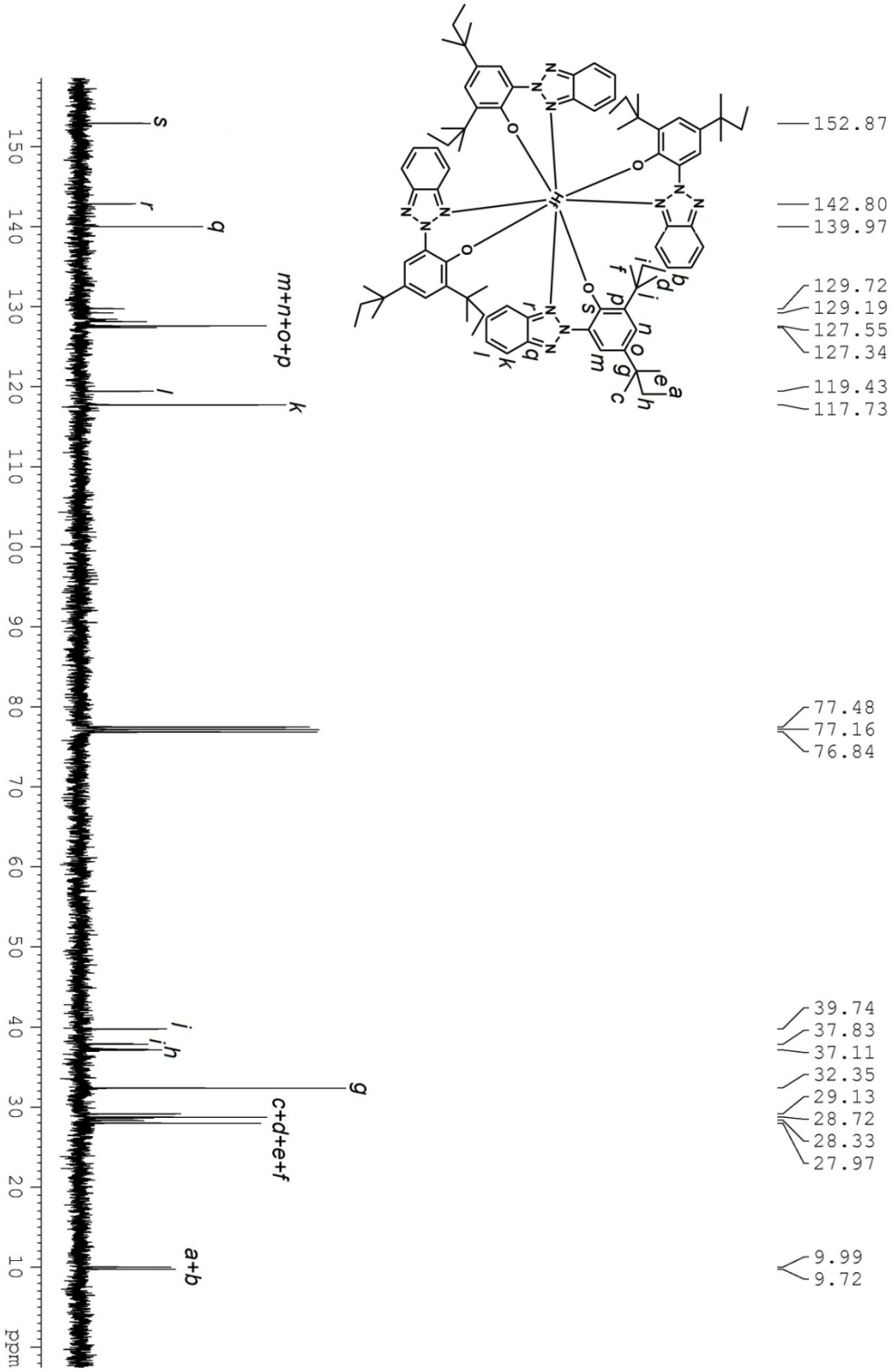

Fig. S26. ^{13}C NMR (125 MHz, $CDCl_3$) of Compound **9**

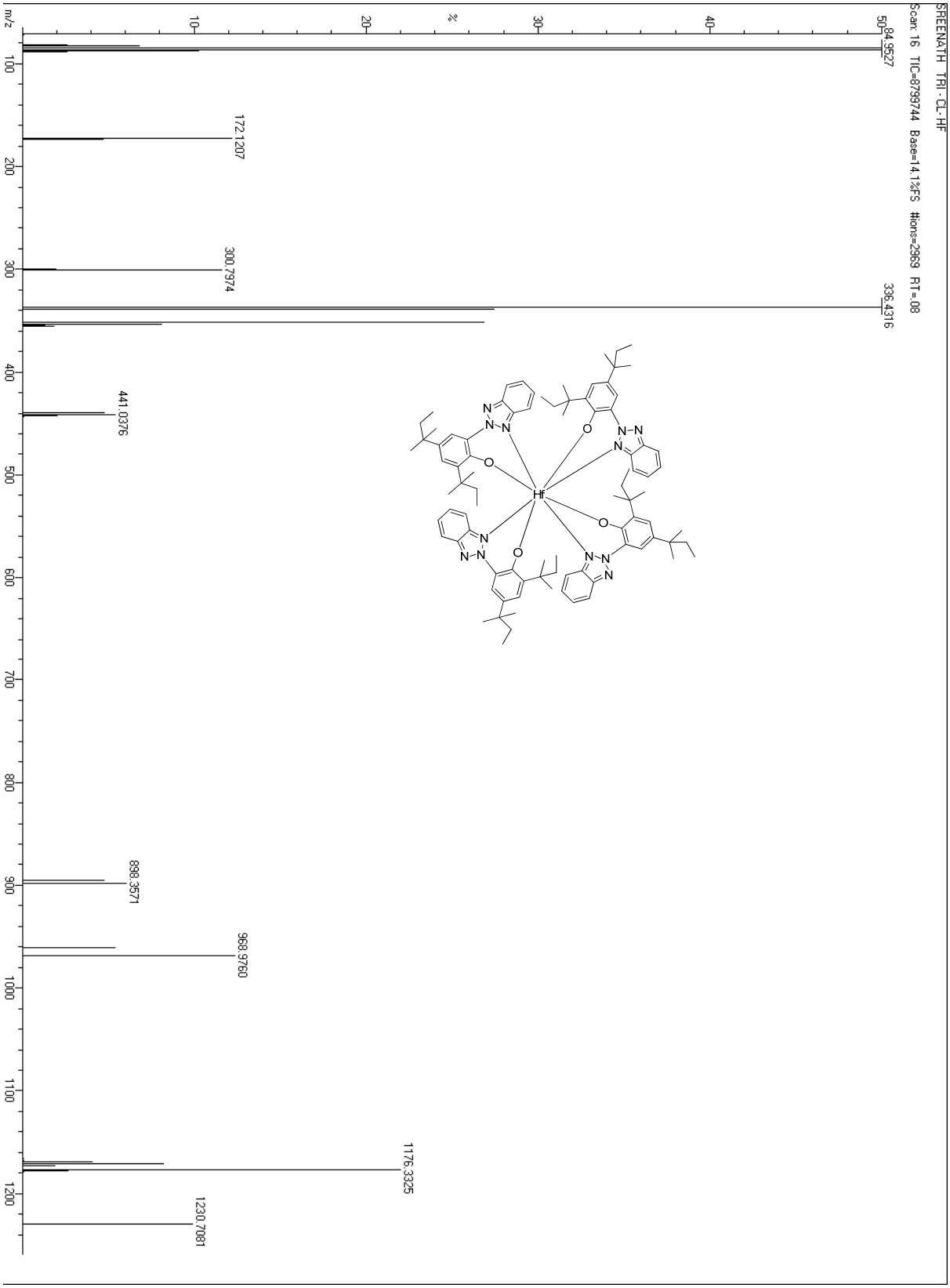

Fig. S27. ESI-Mass Spectrum of Compound **9**

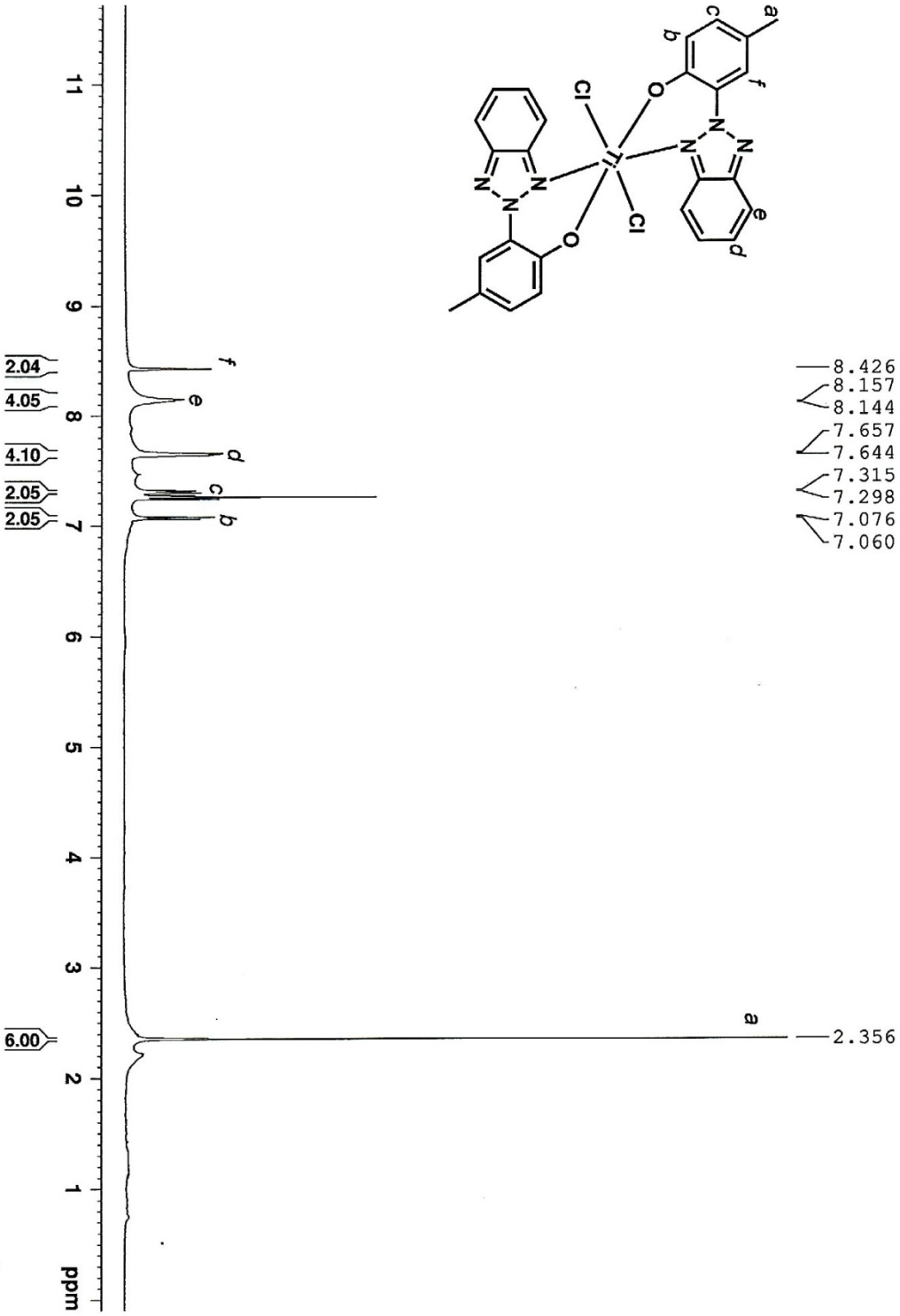

Fig. S28. ^{1}H NMR (500 MHz, $CDCl_3$) of Compound **10**

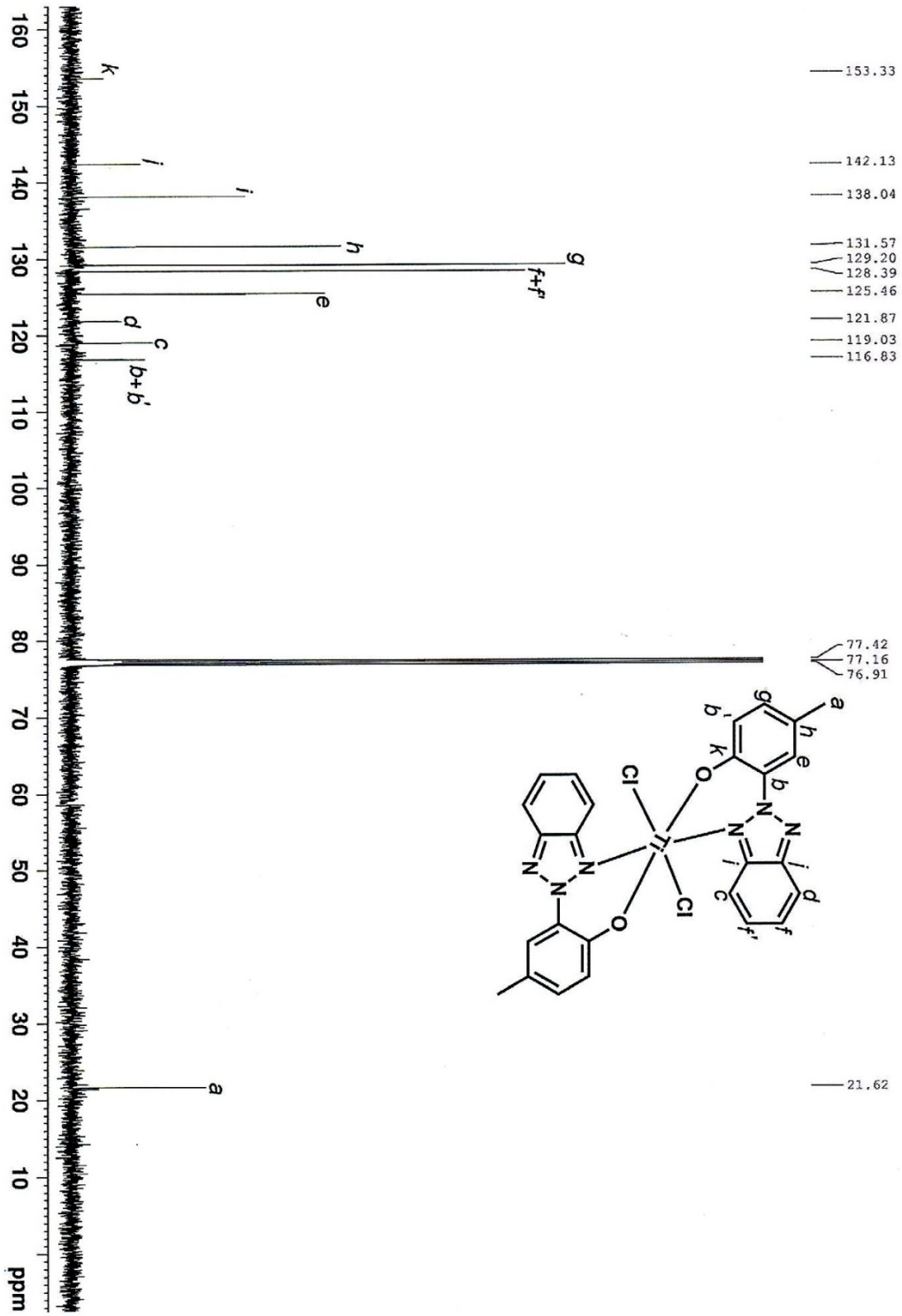

Fig. S29. ^{13}C NMR (125 MHz, $CDCl_3$) of Compound **10**

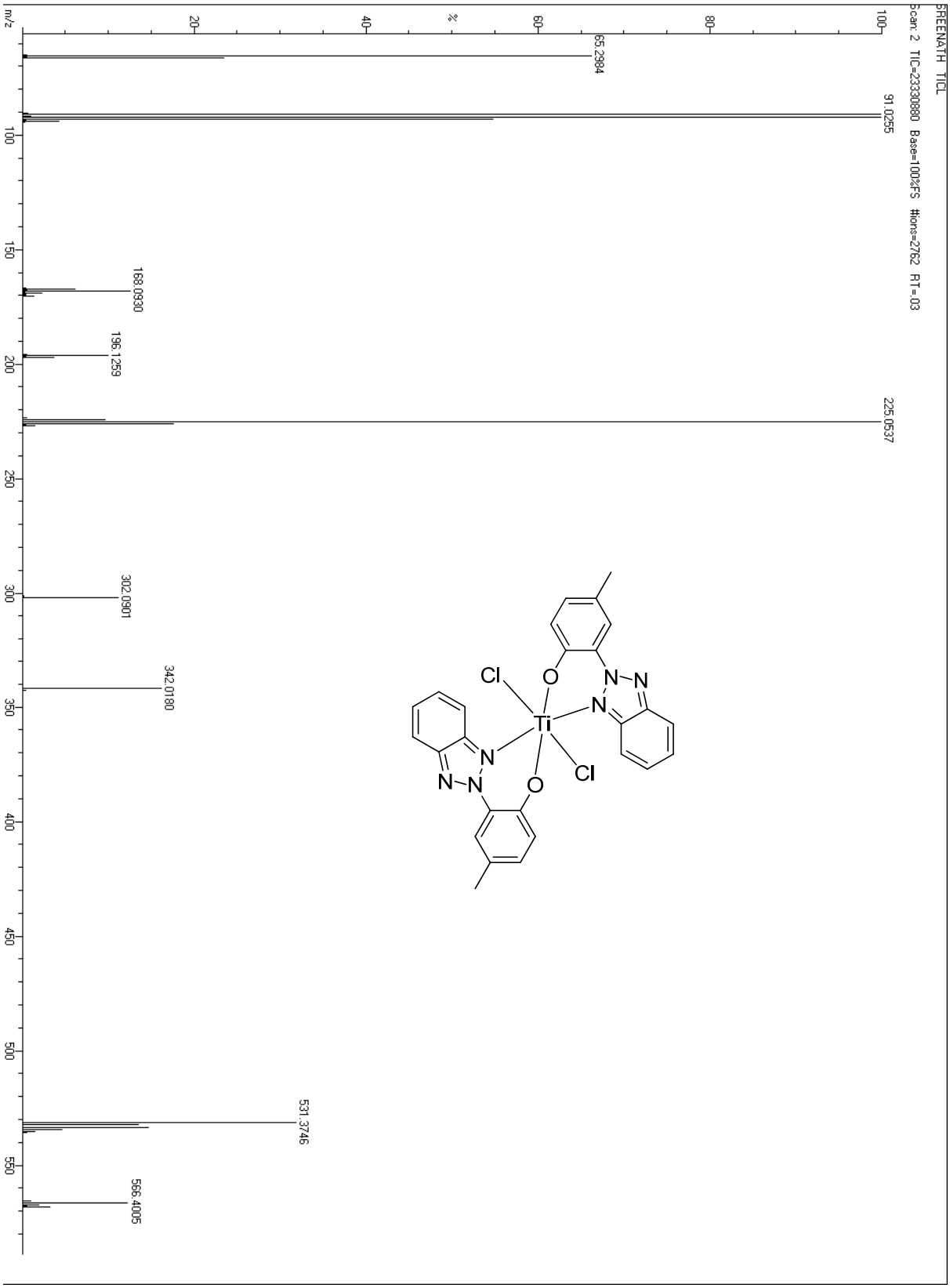

Fig. S30. ESI-Mass Spectrum of Compound **10**

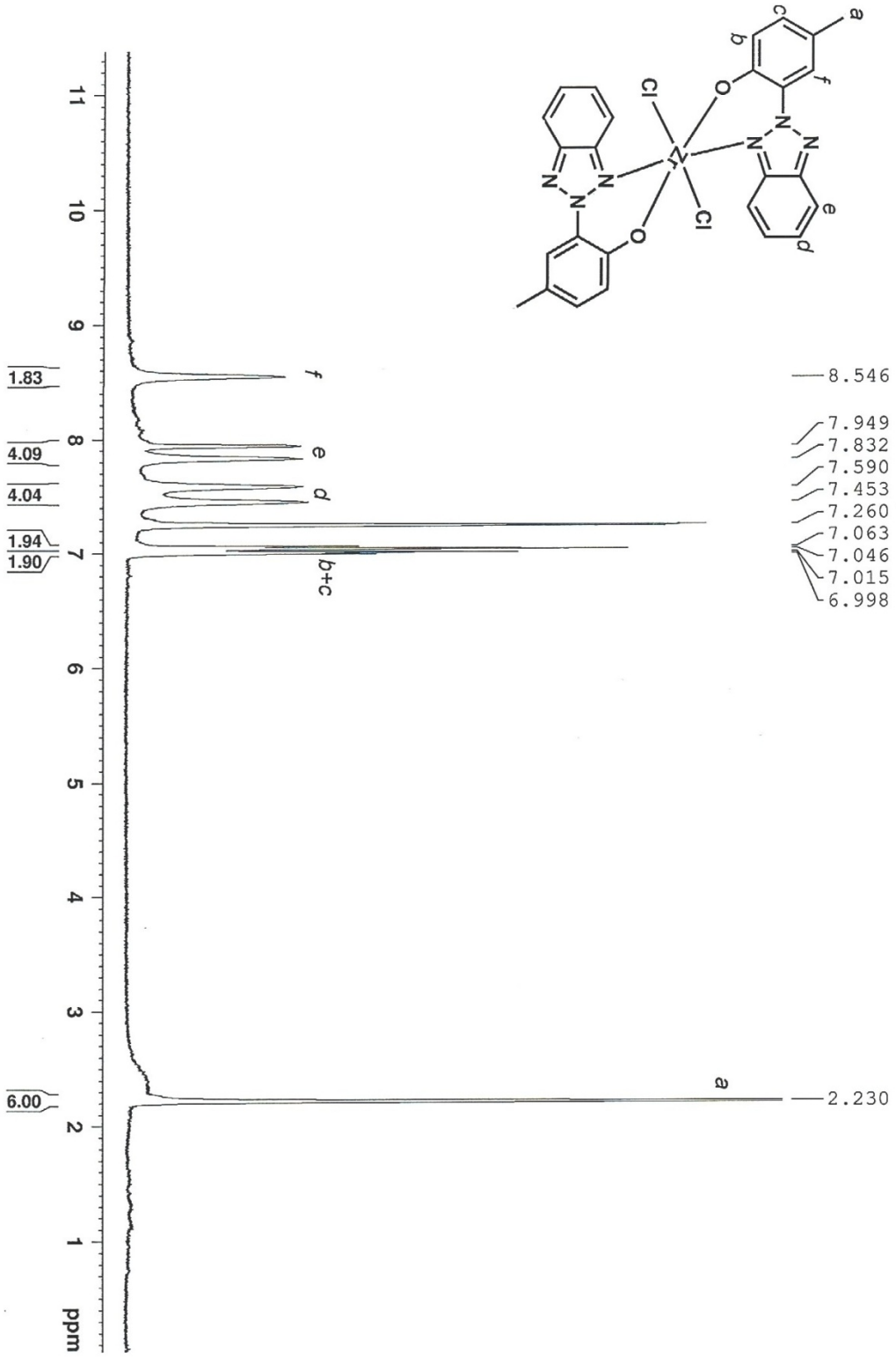

Fig. S31. ^{1}H NMR (500 MHz, $CDCl_3$) of Compound **11**

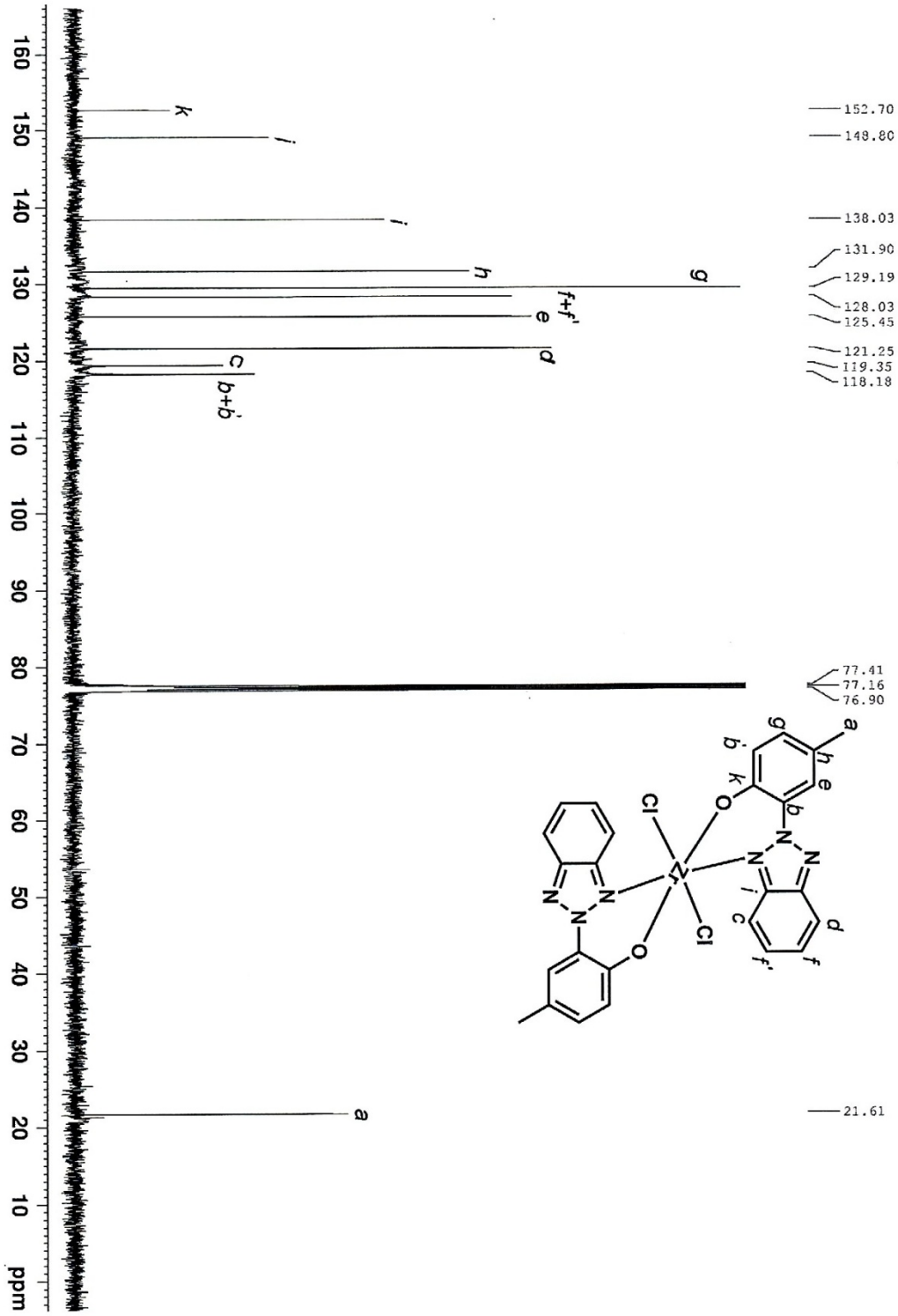

Fig. S32. ^{13}C NMR (125 MHz, $CDCl_3$) of Compound **11**

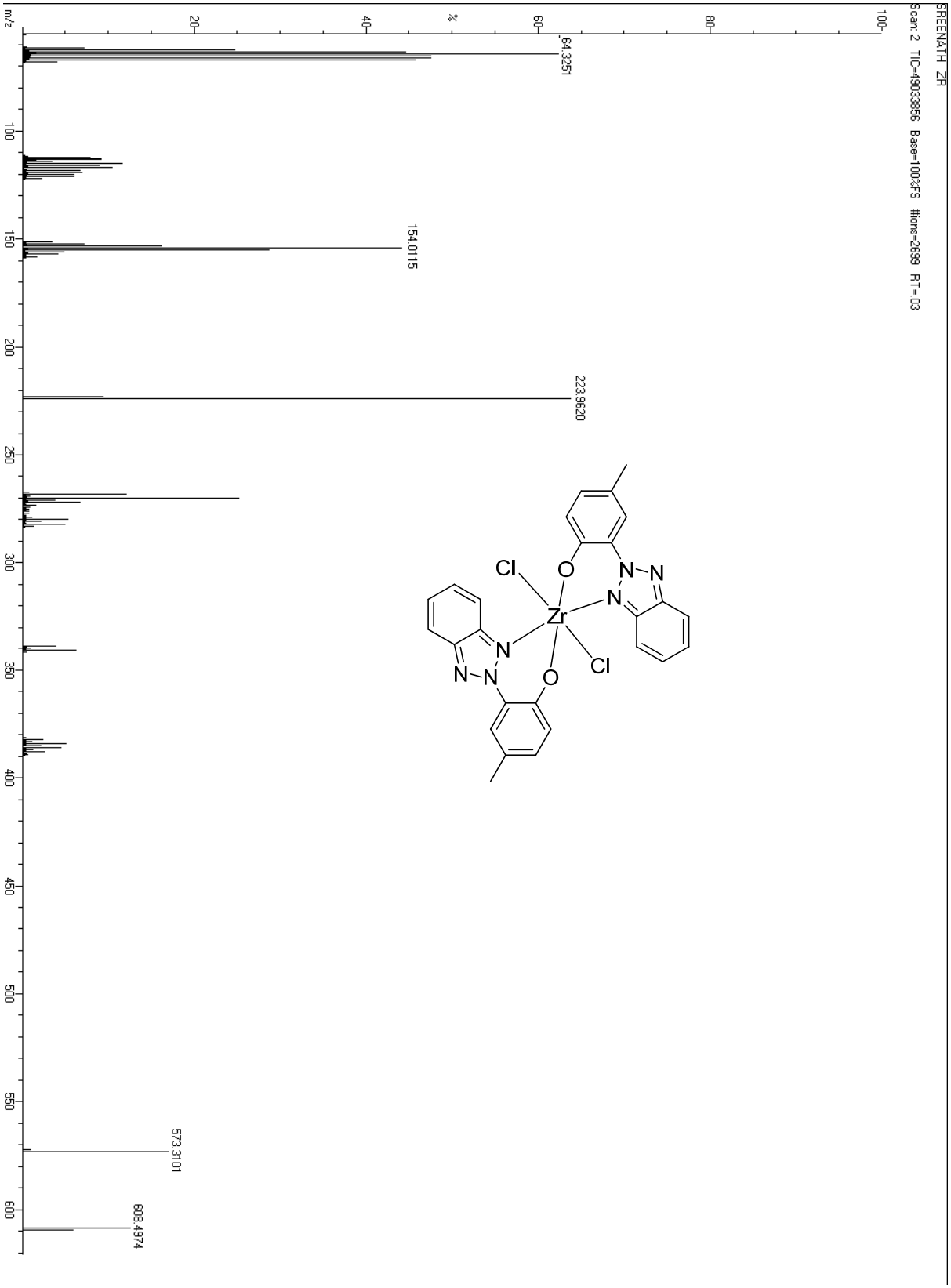

Fig. S33. ESI-Mass Spectrum of Compound **11**

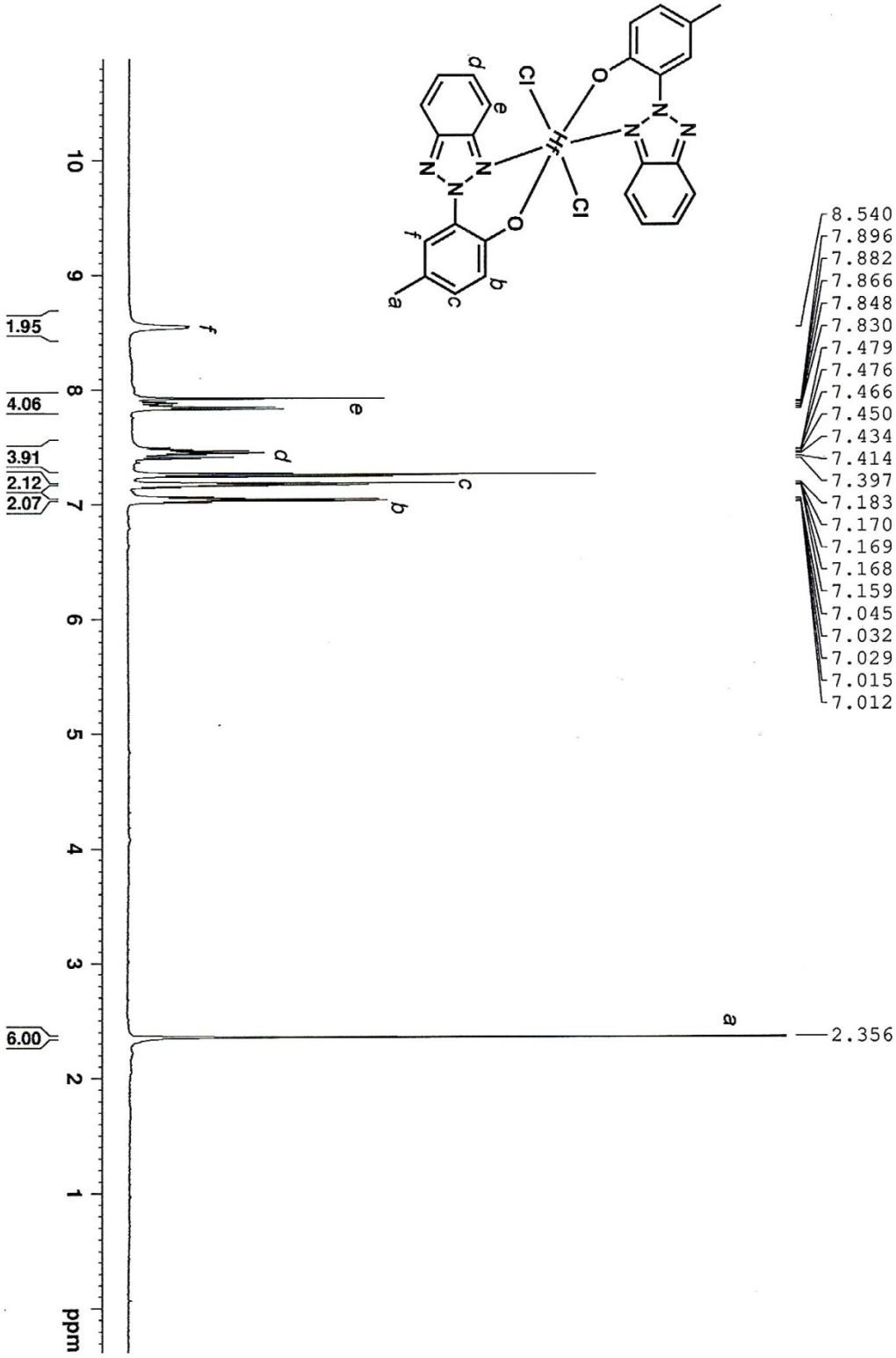

Fig. S34. ^{1}H NMR (500 MHz, $CDCl_3$) of Compound **12**

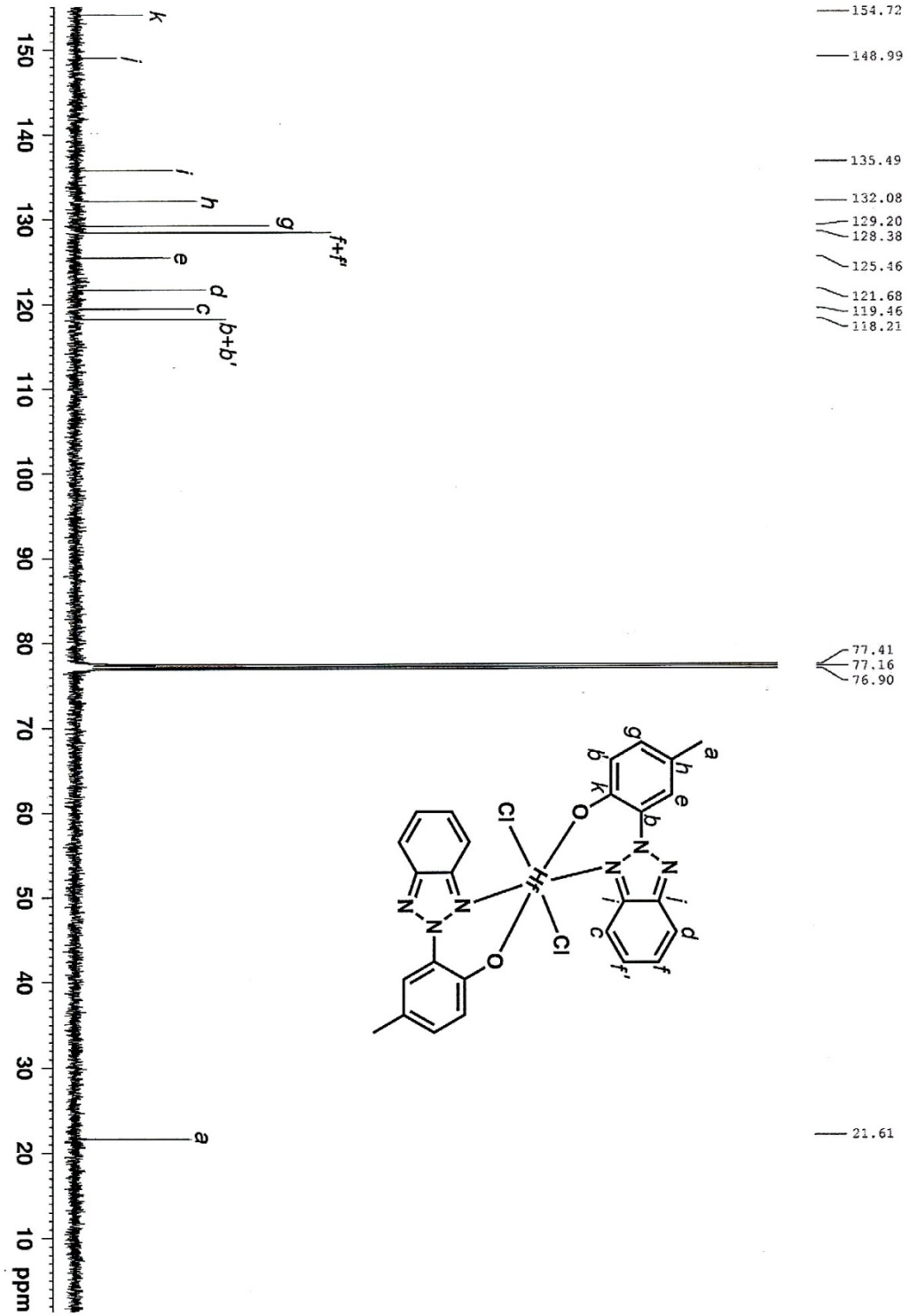

Fig. S35. ^{13}C NMR (125 MHz, $CDCl_3$) of Compound **12**

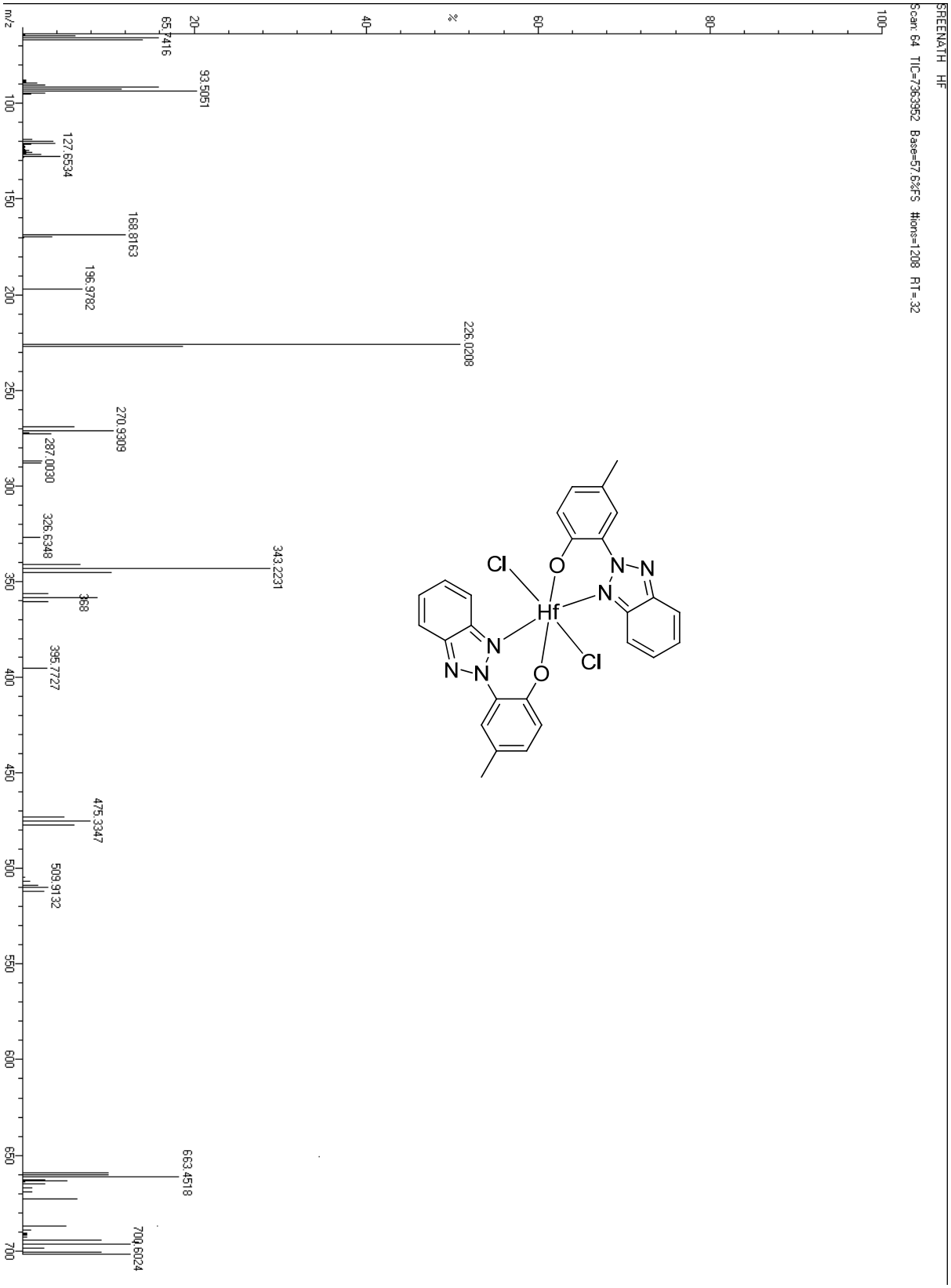

Fig. S36. ESI-Mass Spectrum of Compound **12**

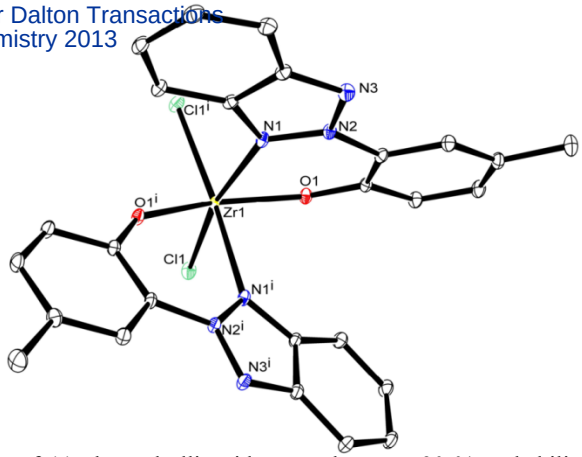

Fig. S37. Molecular structure of **11**; thermal ellipsoids were drawn at 30 % probability level, hydrogen atoms have been omitted for clarity. Selected bond lengths (Å) and angles (◦): Zr(1)–O(1), 1.9702(9), Zr(1)–O(1)i 1.9702(9), Zr(1)–N(1) 2.3731(16), Zr(1)–N(1)i 2.3731, Zr(1)–Cl(1) 2.4135(4), Zr(1)–Cl(1)i 2.4135(4), O(1)–Zr(1)–N(1) 75.30(4), O(1)i–Zr(1)–N(1)i 75.30(4).

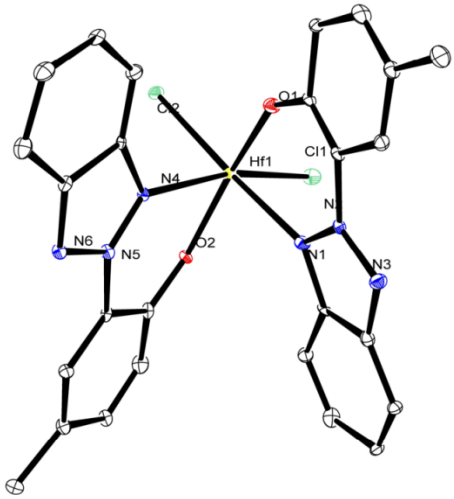

Fig. S38. Molecular structure of **12**; thermal ellipsoids were drawn at 30 % probability level, hydrogen atoms have been omitted for clarity. Selected bond lengths (Å) and angles (◦): Hf(1)–O(1), 1.958(8), Hf(1)–O(2) 1.971(7), Hf(1)–N(1) 2.295(9), Hf(1)–N(4) 2.392(8), Hf(1)–Cl(1) 2.385(4), Hf(1)–Cl(2) 2.403(4), O(1)–Hfi(1)–N(1) 76.6(3), O(2)–Hf(1)–N(4) 76.0(3).

Table I Crystal data for the structures **1**, **4**, **7**, **10**, **11** and **12**

Compounds	**1**	**4**	**7**	**10**	**11**	**12**
Molecular formula	$C_{22}H_{31}N_3O_4Zr$	$C_{73}H_{64}N_{12}O_4Zr$	$C_{73}H_{64}Hf\ N_{12}O_4$	$C_{59}H_{48}Cl_4N_{12}O_4Ti$	$C_{26}H_{20}Cl_2N_6O_2Zr$	$C_{26}H_{20}Cl_2Hf\ N_6O_2$
Formula weight	492.72	1264.58	1351.85	1226.69	610.60	697.87
T/K	173(2) K	173(2) K	173(2) K	173(2) K	173(2) K	173(2) K
Wavelength (Å)	0.71073A	0.71073 A	0.71073 A	0.71073 A	0.71073 A	0.71073 A
Crystal system, Space group	Monoclinic, C2/c	Monoclinic, P2(1)/c	Monoclinic, P2(1)/c	Triclinic, P-1	Monoclinic, C2/c	Monoclinic, Cc
a/ Å	17.9699(8)	12.5037(4)	12.5729(7)	12.0351(5)	18.6144(15)	18.5596(6)
b/ Å	12.6633(6)	30.0814(10)	29.9689(16)	12.7717(6)	10.8807(8)	10.9098(3)
c/ Å	22.2998(10)	17.0526(6)	17.1728(9)	18.3390(8)	15.4550(12)	15.4502(5)
α (°)	90	90	90	103.316(2)	90	90
β (°)	111.613(2)	109.807(2)	109.688(2)	93.616(2)	124.471(3)	124.5010(10)
γ (°)	90	90	90	91.888(2)	90	90
V/ $Å^3$	4717.7(4)	6034.5(4)	6092.4(6)	2734.3(2)	2580.6(3)	2578.15(14)
Z, Calculated density (g cm^{-3})	8, 1.387 Mg/m^3	4, 1.392 Mg/m^3	4, 1.474 Mg/m^3	2, 1.490 Mg/m^3	4,1.572 Mg/m^3	4, 1.798 Mg/m^3
Absorption coefficient(mm^{-1})	0.497 mm^-1	0.246 mm^-1	1.776 mm^-1	0.549 mm^-1	0.670 mm^-1	4.290 mm^-1
θ range/°	2.43 to 28.47	1.89 to28.55	1.85 to 28.38	1.64 to 30.44	2.29 to 28.60	2.29 to 28.34
Reflections collected/unique	16386	44575	45634	40307	8798	8579
Independent reflections	5374	13796	14989	15262	3204	3569
Data/restraints/parameters	5374/0/ 272	13796 / 0 / 818	14989 / 5 / 818	15262 / 0 / 735	3204 / 0 / 169	3569 / 206 / 325
Goodness-of-fit on F2	1.018	1.081	1.177	1.019	1.041	1.044
Final R indices [$I > 2\sigma(I)$]	R1 = 0.0421, wR2 = 0.1039	R1 = 0.0688, wR2 = 0.1635	R1 = 0.0358, wR2 = 0.0735	R1 = 0.0401, wR2 = 0.0917	R1 = 0.0235, wR2 = 0.0624	R1 = 0.0124, wR2 = 0.0322
R indices (all data)	R1 = 0.0491, wR2 = 0.1104	R1 = 0.0839, wR2 =0.1724	R1 = 0.0456, wR2 = 0.0772	R1 = 0.0628, wR2 = 0.1017	R1 = 0.0257, wR2 = 0.0639	R1 = 0.0127, wR2 = 0.0324
Max. and min. transmission	0.9071 and 0.8453	0.9570 and 0.9410	0.7766 and 0.6652	0.9076 and 0.8750	0.8777and 0.7994	0.4808 and 0.3406

$R_1 = \sum|F_0| - |F_c|/\sum|F_0|$, $wR_2 = [\sum (F_0^2 - F_c^2)^2/\sum w(F_0^2)^2]^{1/2}$

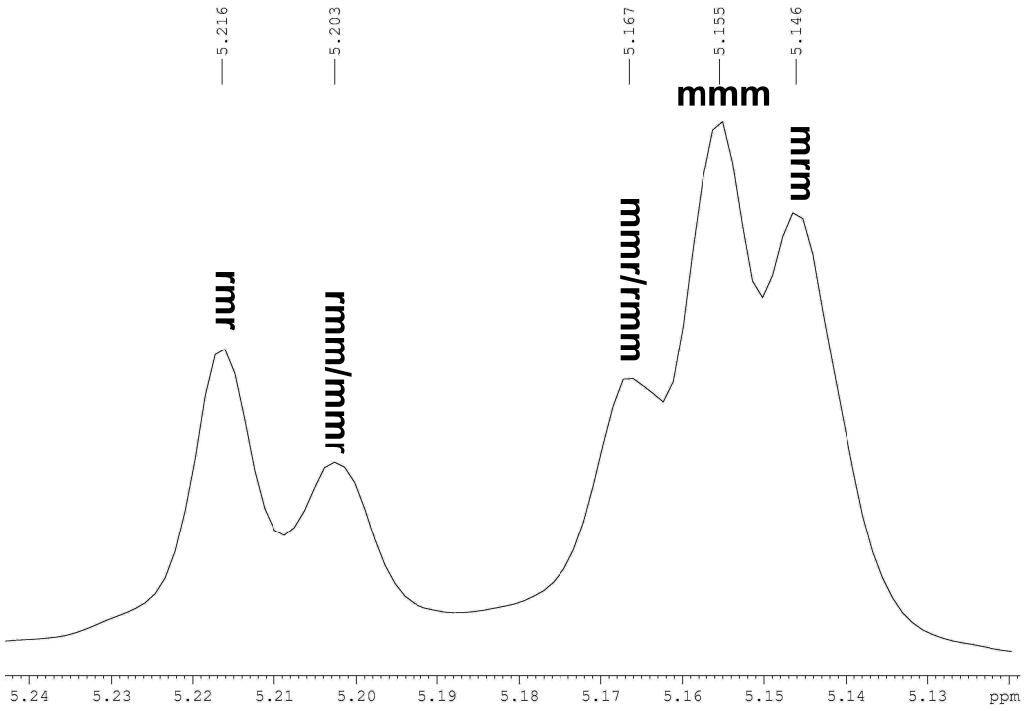

Fig. S39. Homonuclear decoupled ^{1}H NMR (500 MHz, CDCl 3) spectrum of the methine region of PLA obtained using **1** (Table 2, Entry 1).

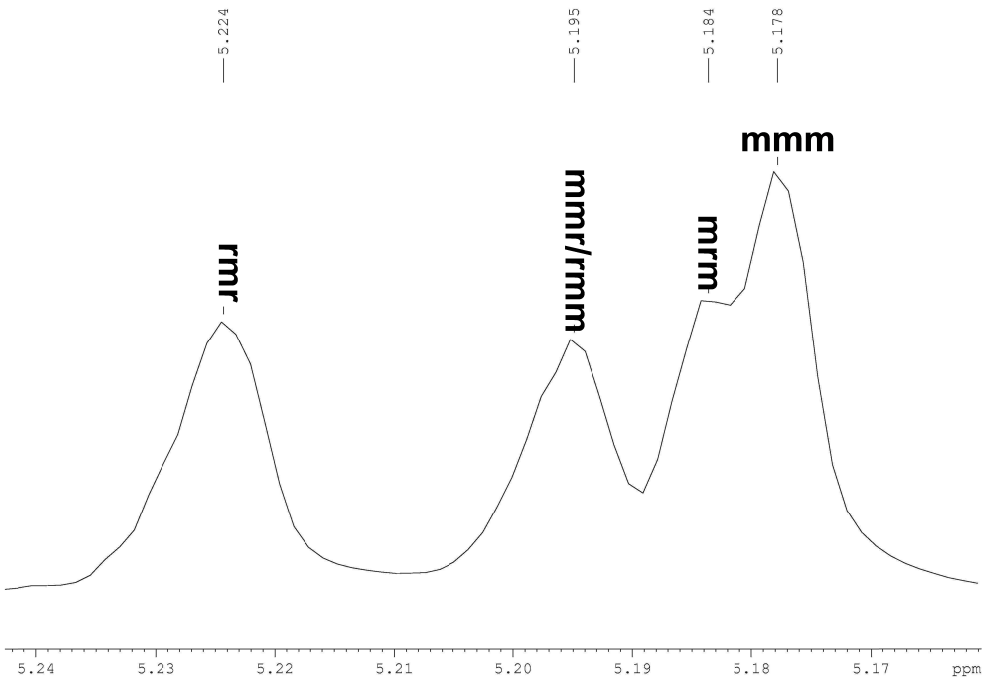

Fig. S40. Homonuclear decoupled ^{1}H NMR (500 MHz, $CDCl_3$) spectrum of the methine region of PLA obtained using **4** (Table 2, Entry 6).

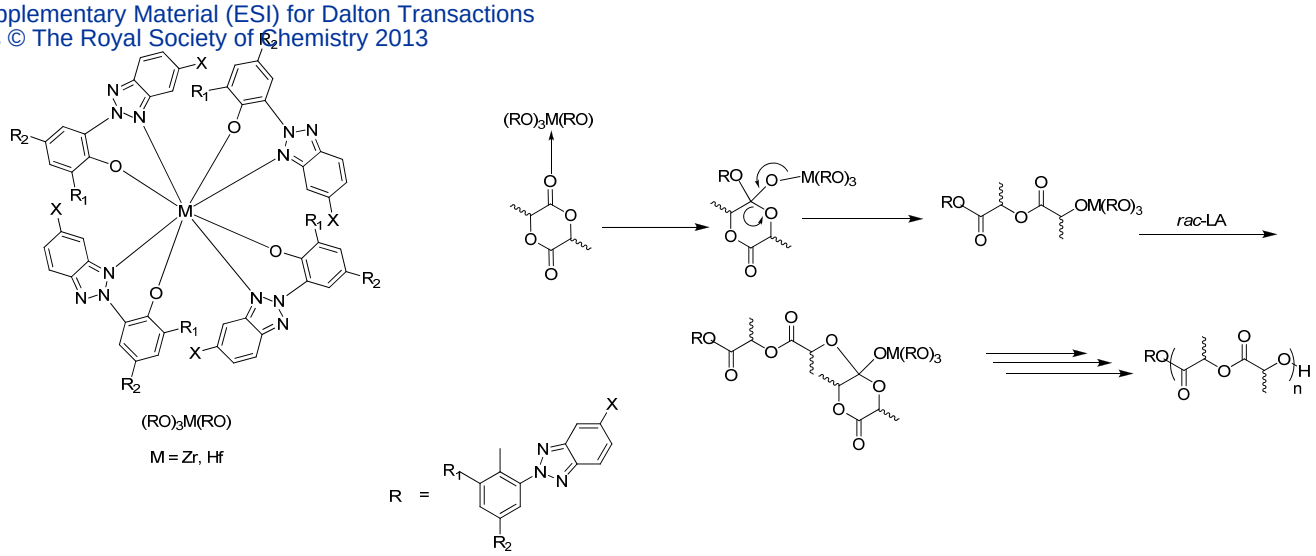

Scheme I Mechanism of ring-opening polymerization initiated by complexes **4–9**

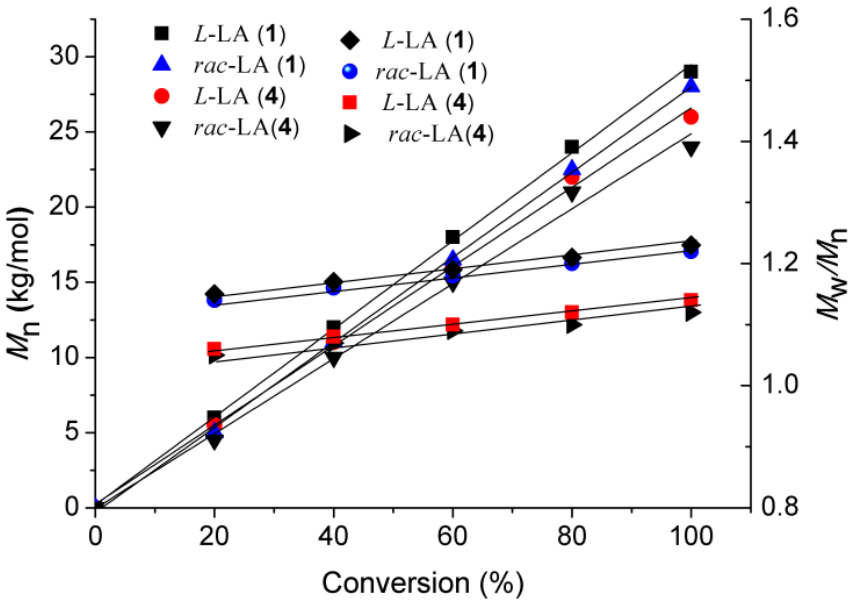

Fig. S41. Plot of M_n and M_w/M_n vs. % conversion for *L*–LA and *rac*–LA polymerization at 140 °C using **1** and **4**.

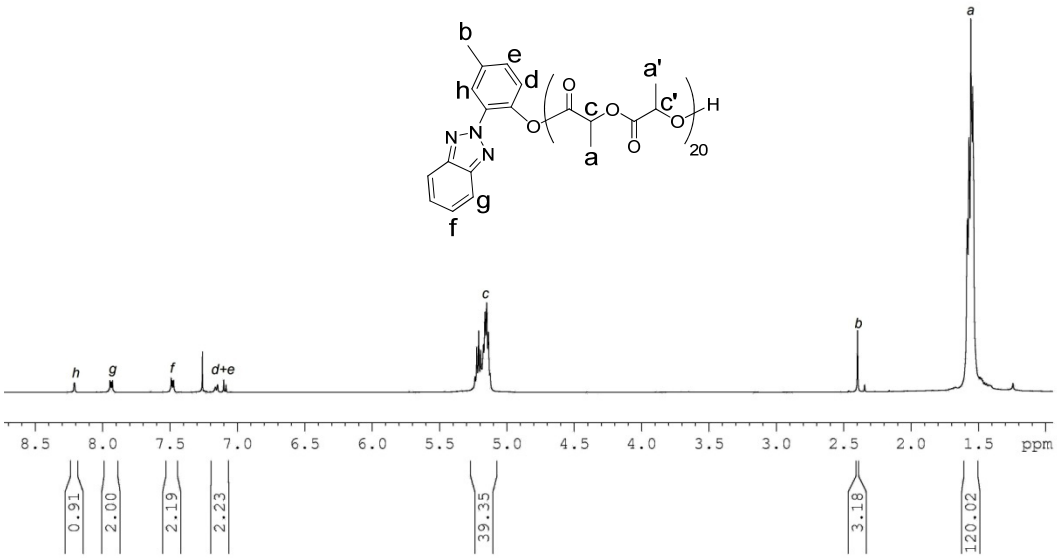

Fig. S42. ^{1}H NMR spectrum (500 MHz, $CDCl_3$) of the crude product obtained from a reaction between *rac*–LA and **4** in 20:1 ratio at 140 °C.

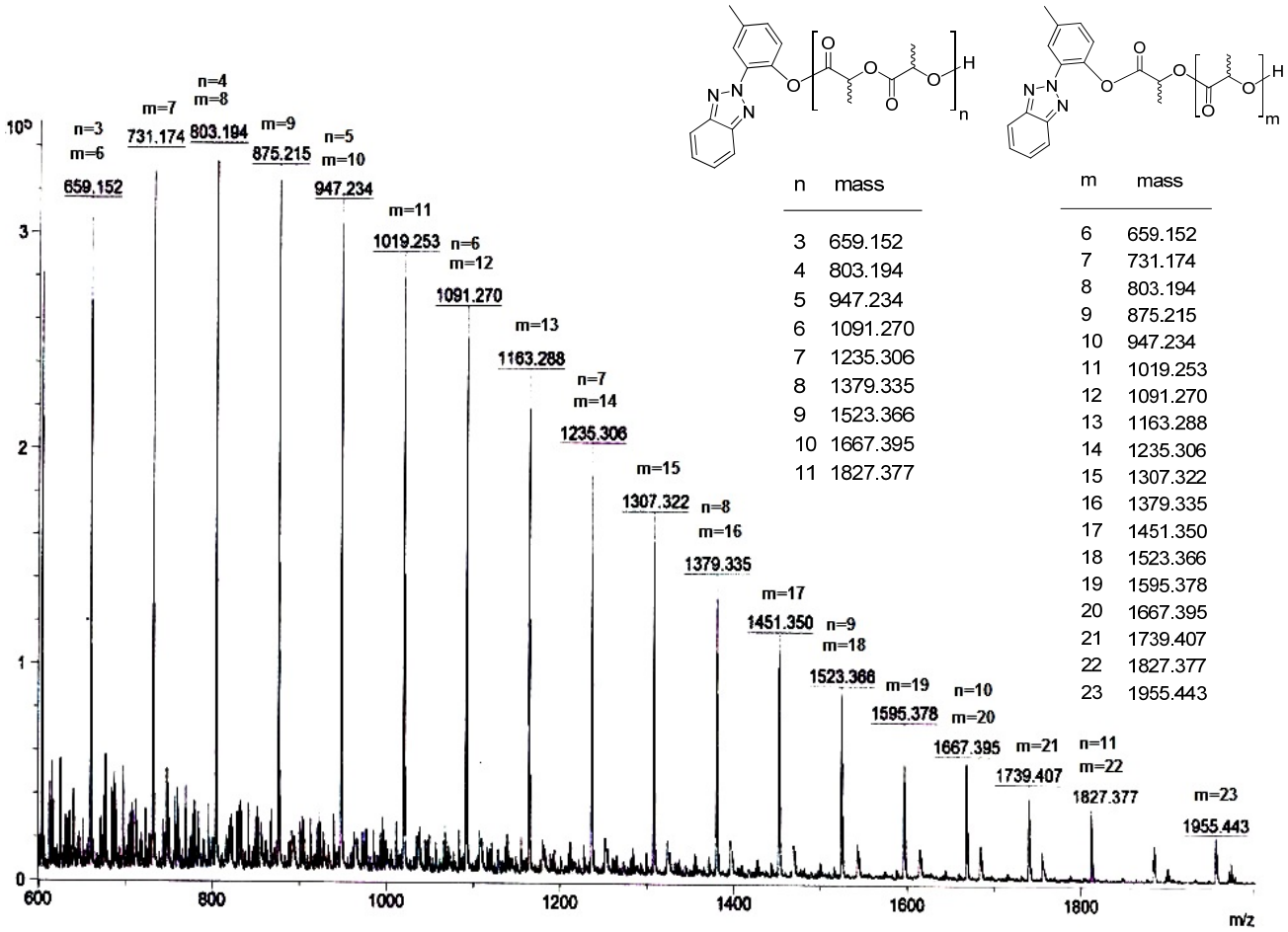

n	mass
3	659.152
4	803.194
5	947.234
6	1091.270
7	1235.306
8	1379.335
9	1523.366
10	1667.395
11	1827.377

m	mass
6	659.152
7	731.174
8	803.194
9	875.215
10	947.234
11	1019.253
12	1091.270
13	1163.288
14	1235.306
15	1307.322
16	1379.335
17	1451.350
18	1523.366
19	1595.378
20	1667.395
21	1739.407
22	1827.377
23	1955.443

Fig. S43. MALDI-TOF spectrum of the crude product obtained from a reaction between *rac*–LA and **4** in 20:1 ratio at 140 °C.

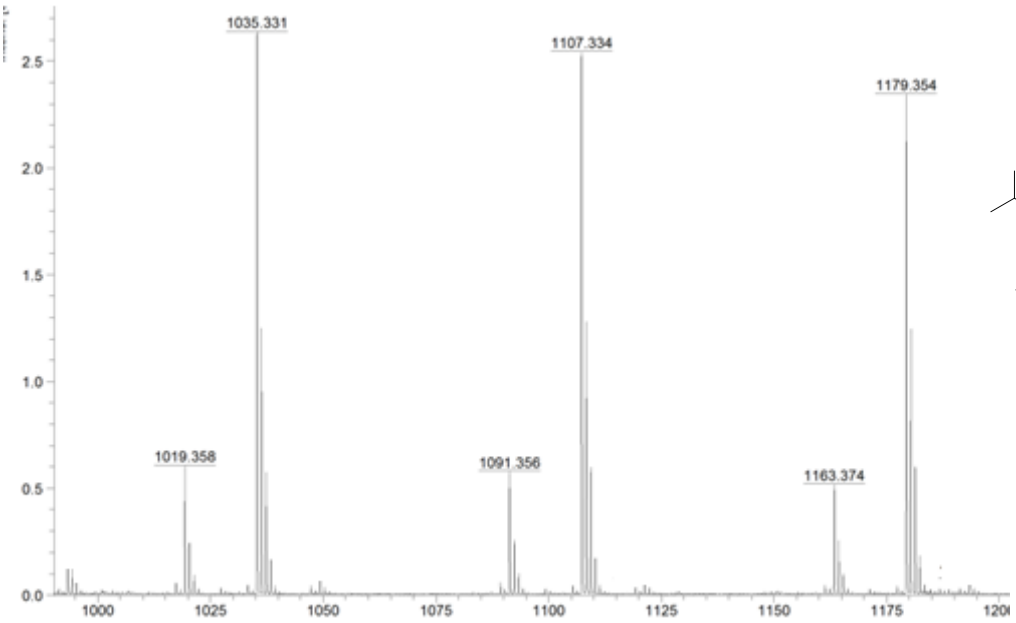

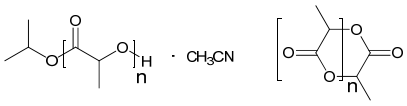

n	mass
13	1035.331
14	1107.334
15	1179.354

n	mass
14	1019.358
15	1091.356
16	1163.374

Fig. S44. Intramolecular transesterification products present in MALDI-TOF spectrum of the crude product obtained from a reaction between *rac*-LA and complex **1** in 20:1 ratio at 140 °C.

1. Polymerization Details

1.1 Determination of molecular weights

Data concerning molecular weights (M_n) and the MWDs (M_w/M_n) of the polymer samples obtained by the ring-opening polymerization (ROP) of lactides (LA) and epoxides were determined by using a GPC instrument with Waters 510 pump and Waters 410 differential refractometer as the detector. Three columns namely WATERS STRYGEL-HR5, STRYGEL-HR4 and STRYGEL-HR3 each of dimensions (7.8 × 300 mm) were connected in series. Measurements were done in THF at 27 °C. In the case of LA number average molecular weights (M_n) and polydispersity (M_w/M_n) (MWDs) of polymers were measured relative to polystyrene standards with Mark-Houwink corrections.

Molecular weights (M_w) and the MWDs (M_w/M_n) of ethylene samples were determined by GPC instrument with Waters 510 pump and Waters 2414 differential refractometer as the detector. The column namely WATERS STRYGEL-HR4 of dimensions (4.6 × 300 mm) was connected during the experiment. Measurements were done in tri-chloro benzene (TCB). Number average molecular weights (M_n) and molecular weight distributions (MWDs) of polymers were measured relative to polystyrene standards.

1.2 Polymerization Kinetics

Bulk polymerization using **1, 2**, **5**, **8** and **11** were carried out at 140 °C under an argon atmosphere. At appropriate interval of time, 0.2 mL aliquots were removed from the reaction mixture, quenched and analysed by ^{1}HNMR. The [*rac*-LA]$_o$ /[*rac*-LA]$_t$ ratio was calculated by integration of the peak corresponding to the methine proton for the monomer and polymer. Apparent rate constant were obtained from the slopes of the best-fit lines.

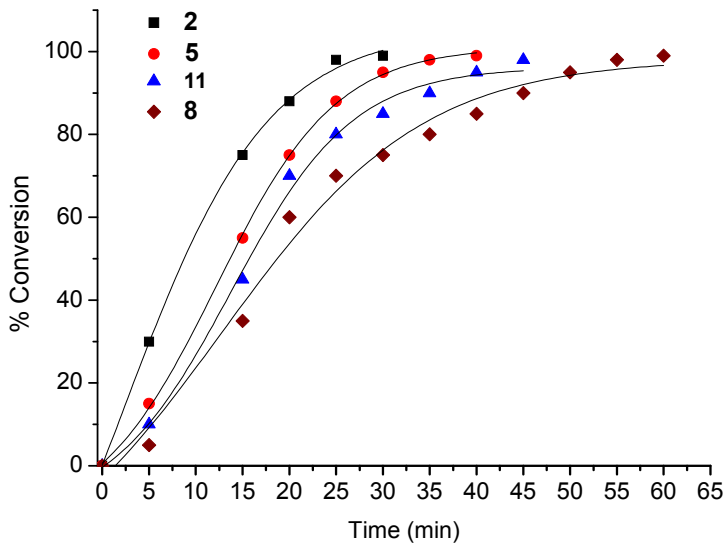

Fig. S45. *rac*-LA conversion *vs* time plot using **2**, **5**, **8** and **11**: [*rac*-LA]$_o$/[Cat]$_o$ = 200 at 140 °C.

Table II Computed Mulliken Net charges (Q/e) on various atoms of metal complexes **1**, **4**, **7**, **10**, **11** and **12**.

Complex	Positions	Mulliken Charge (Q/e)	Complex	Positions	Mulliken Charge (Q/e)
	O1	–0.834		O1	–0.773
	O2	–0.873		O2	–0.775
	O3	–0.861		O3	–0.767
1	O4	–0.858	**4**	O4	–0.769
	N1	–0.306		N1	–0.301
	N2	–0.056		N4	–0.274
	N3	–0.261		N7	–0.273
	Zr	1.965		Zr	1.714
	O1	–0.802		O1b	–0.587
	O2	–0.801		O2b	–0.591
	O3	–0.795		Cl1b	–0.126
7	O4	–0.793	**10**	Cl2b	–0.425
	N11	–0.276		N1b	–0.285
	N14	–0.052		N4b	–0.054
	N17	–0.273		N6b	–0.250
	Hf	1.841		Ti	0.453
	O1	–0.754		O1	–0.790
	O1^{i}	–0.754		O2	–0.778
	Cl1	–0.275		Cl1	–0.303
11	Cl1^{i}	–0.275	**12**	Cl2	–0.296
	N1	–0.351		N1	–0.348
	N2	0.055		N2	0.031
	N3	–0.251		N3	–0.287
	Zr	1.229		Hf	1.351

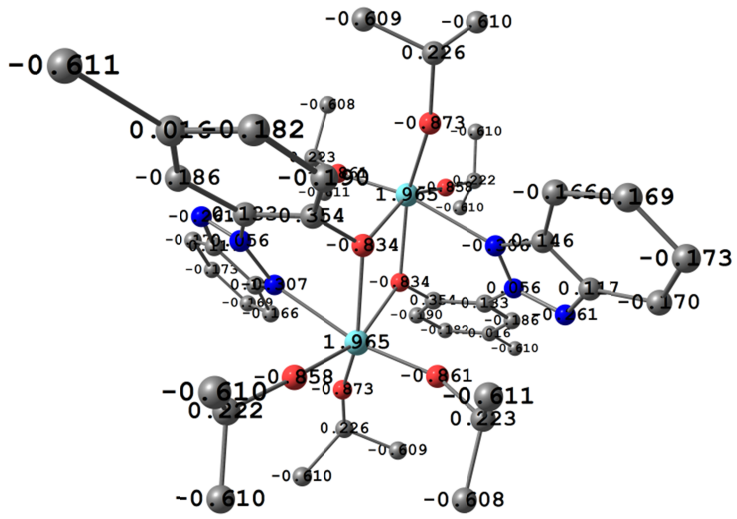

Complex **1**

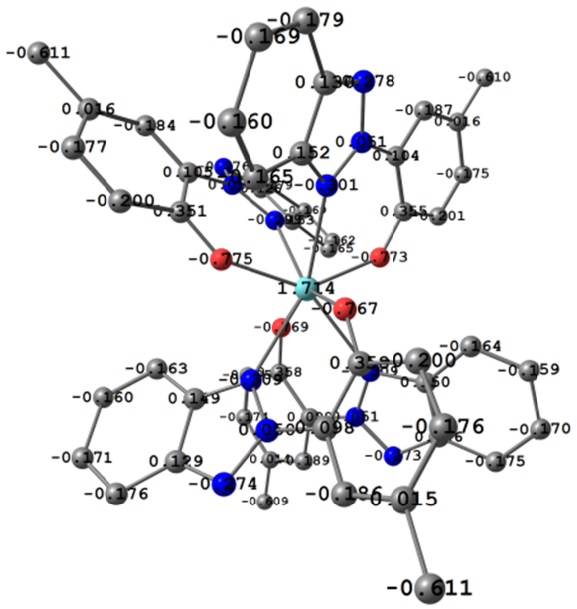

Complex **4**

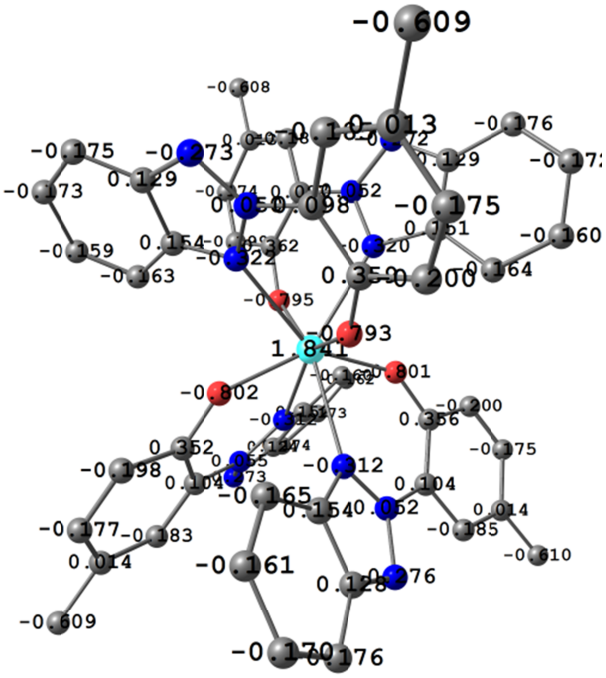

Complex **7**

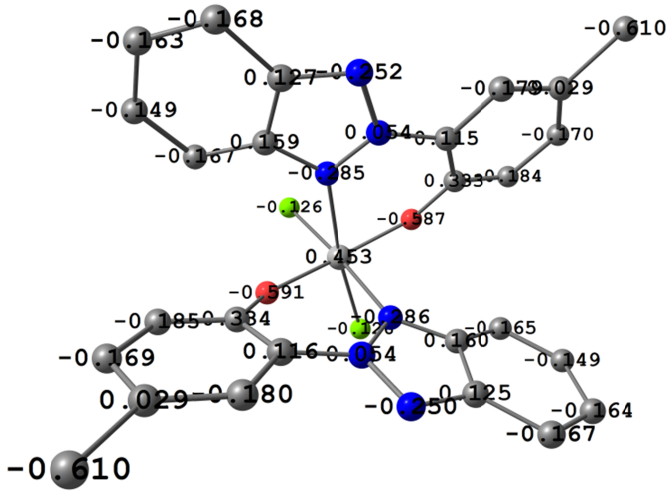

Complex **10**

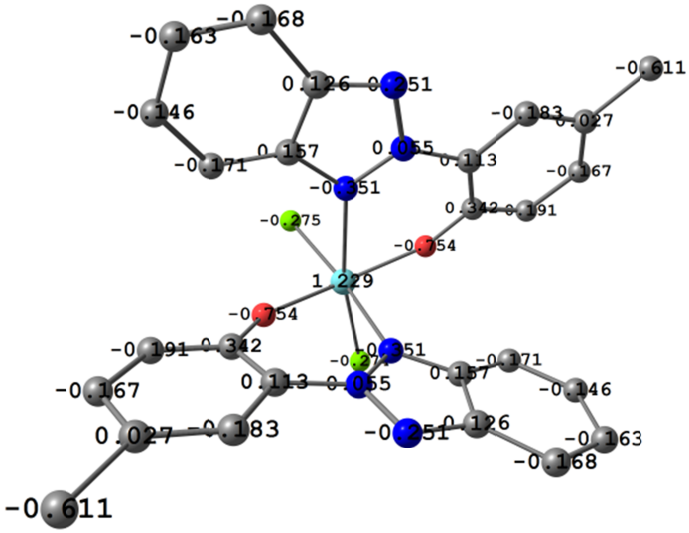

Complex **11**

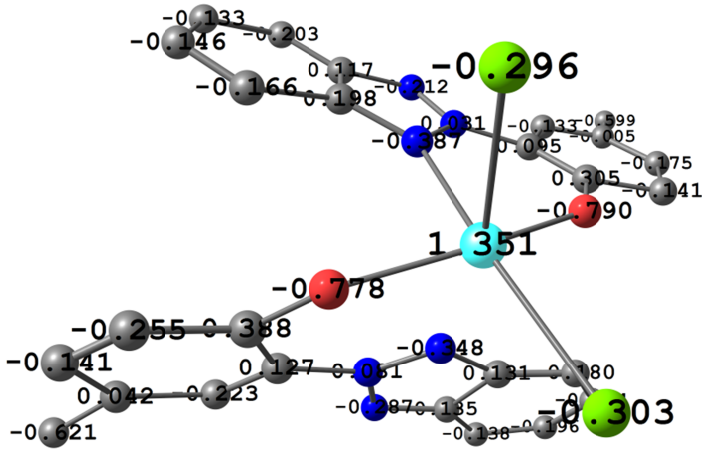

Complex **12**

Fig. S46. Mulliken partial charges of complexes **1**, **4**, **7**, **10**, **11** and **12**.

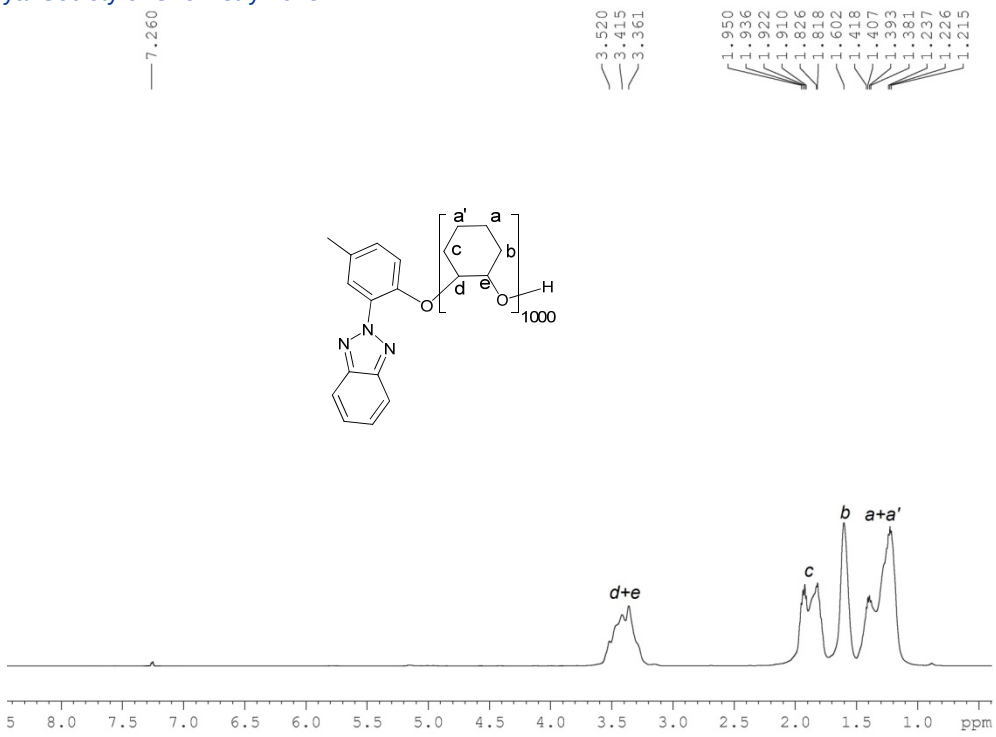

Fig. S47. ^{1}H NMR spectrum (500 MHz, $CDCl_3$) of the crude product obtained from a reaction between CHO and **1** in 1000:1 ratio at 100 °C.

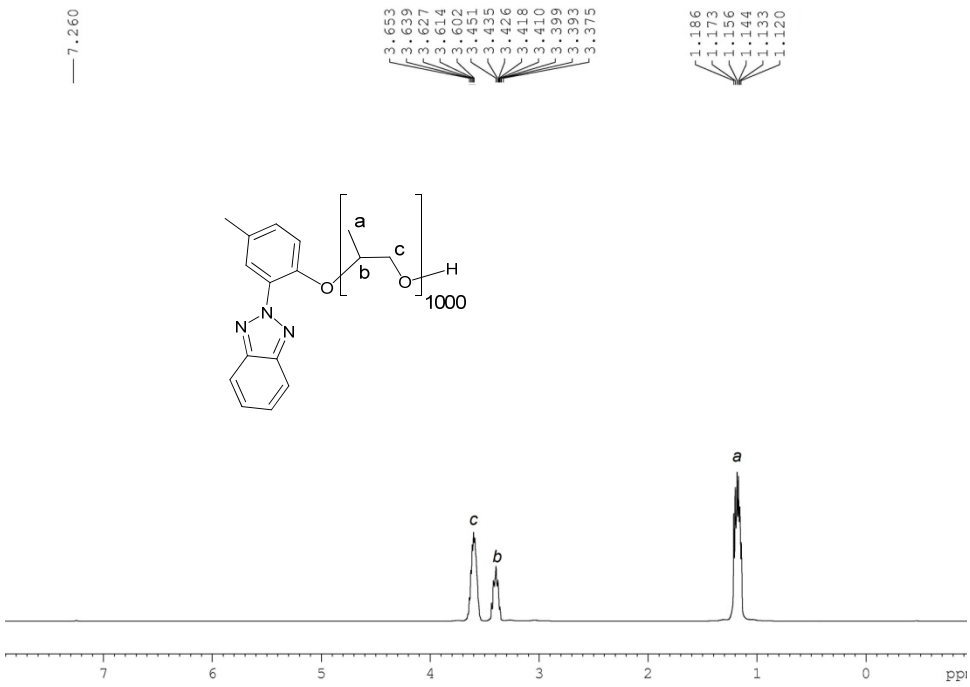

Fig. S48. ^{1}H NMR spectrum (500 MHz, $CDCl_3$) of the crude product obtained from a reaction between PO and **1** in 1000:1 ratio at 30 °C.

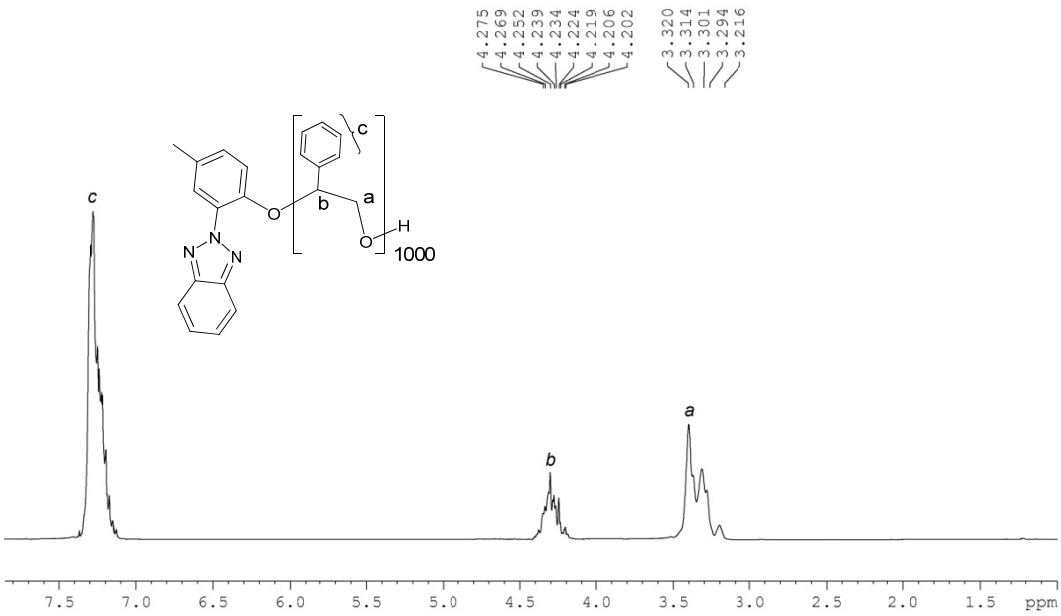

Fig. S49. ^{1}H NMR spectrum (500 MHz, $CDCl_3$) of the crude product obtained from a reaction between SO and **1** in 1000:1 ratio at 130 °C.

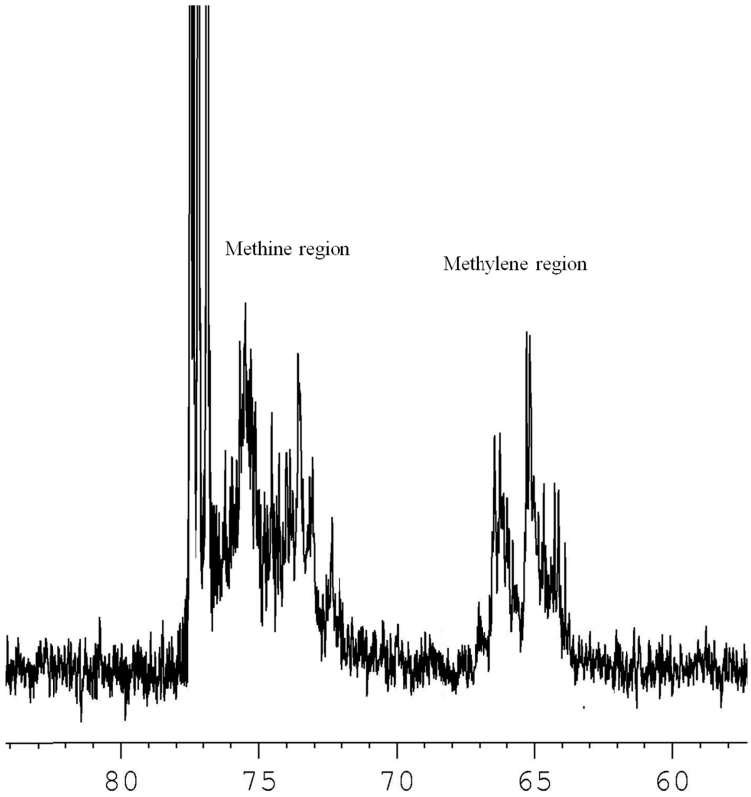

Fig. S50. C^{13} {^{1}H} NMR spectrum (400 MHz, $CDCl_3$) showing the methine and methylene carbons for the regioirregular polymer obtained from a reaction between *rac*-PO and **1** in 1000:1 ratio at 30 °C.

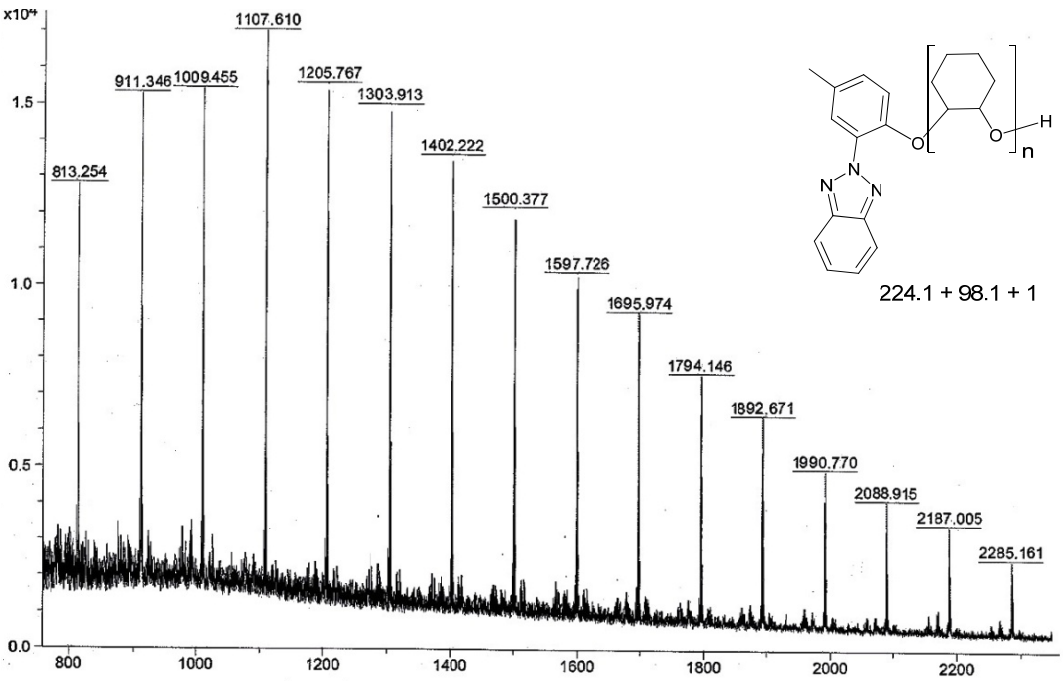

n	mass
6	813.254
7	911.346
8	1009.455
9	1107.610
10	1205.767
11	1303.913
12	1402.222
13	1500.377
14	1597.726
15	1695.974
16	1794.146
17	1892.671
18	1990.770
19	2088.915
20	2187.005
21	2285.161

Fig. S51. MALDI-TOF spectrum of the crude product obtained between a reaction of CHO and complex **1** in 1000:1 ratio at 100 °C.

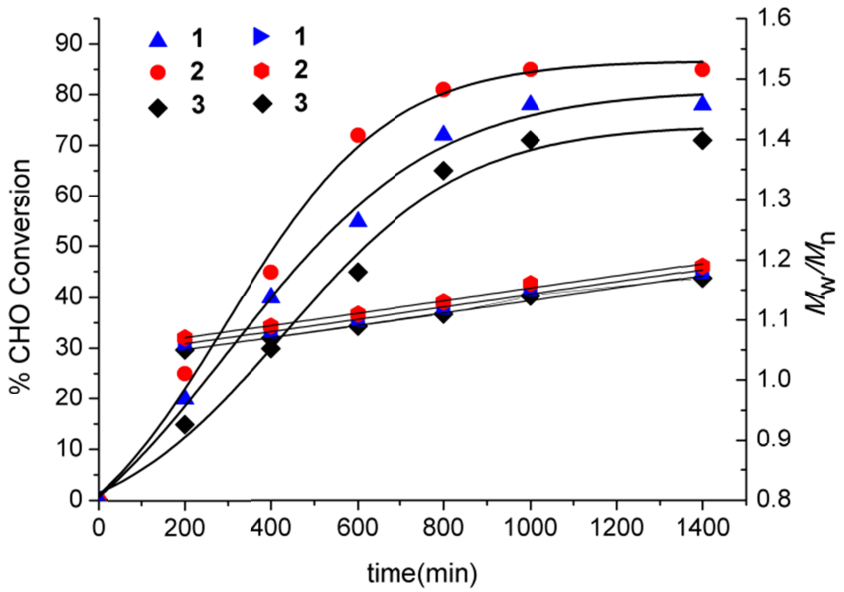

Fig. S52. Plot of % Conversion and M_w/M_n vs. time (min) for CHO polymerization at 100 °C using **1**, **2** and **3**.

Table III Data for the polymerization of ethylene catalyzed by complexes **1−12** with **MAO**

entry	Cat.	MAO:Cat	Yield[a]	Activity[b]	M_n[c] (kg/mol)	M_w/M_n
1	**1**	500	1.2	4.3	80.5	2.1
2	**1**	1000	1.8	7.0	140.1	2.8
3	**1**	1500	1.1	4.6	129.2	2.2
4	**2**	500	1.0	4.9	47.2	2.2
5	**2**	1000	1.5	7.5	118.0	2.5
6	**2**	1500	1.1	5.4	62.0	1.9
7	**3**	500	1.2	5.9	55.1	3.5
8	**3**	1000	1.2	6.0	111.5	2.5
9	**3**	1500	1.0	5.0	66.0	2.2
10	**4**	1000	0.8	3.2	87.4	2.6
11	**5**	1000	5.5	3.3	84.8	2.4
12	**6**	1000	5.3	3.1	76.8	3.1
13	**7**	1000	0.7	3.0	90.4	2.9
14	**8**	1000	4.8	3.0	82.6	2.7
15	**9**	1000	4.5	2.8	71.3	2.9
16	**10**	1000	2.4	5.4	102.1	3.7
17	**11**	1000	2.3	5.6	107.0	3.7
18	**12**	1000	1.5	4.1	80.6	4.8

All experiments were performed in toluene at MAO:catalyst ratio = 1000, unless otherwise indicated. Ethylene pressure = 8 atm, 80 °C for 30 min, catalyst = 50 mg, solvent = 45 mL. [a] g of PE obtained after 30 min. [b]A = Activity in (g PE/mol cat × h) ×10^4. [c]Determined by GPC in 1,2,4-$C_6Cl_3H_3$ vs narrow polystyrene standards.

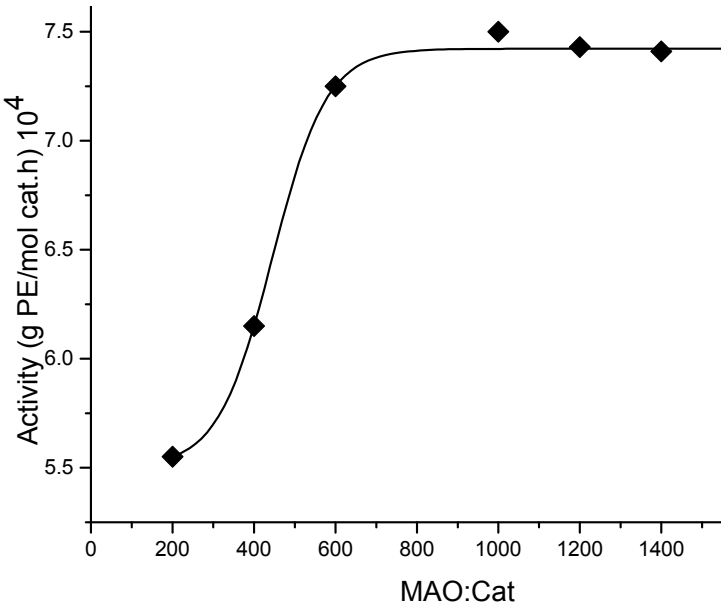

Fig. S53. Activity obtained in the polymerization of ethylene using **2**.